Status and Trends of Groundwater Dependent Vegetation in Relation to Climate and Shallow Groundwater in the Harney Basin, Oregon

Christine M. Albano[1]

Blake Minor[1]

Zach Freed[2]

Justin L. Huntington[1]

March 2020

Publication No. 41280

prepared by

[1]Division of Hydrologic Sciences, Desert Research Institute

[2]The Nature Conservancy in Oregon

prepared for

The Nature Conservancy in Oregon

Contract ORFO-090418-aa01

THIS PAGE INTENTIONALLY LEFT BLANK

ABSTRACT

Shallow groundwater beneath the alluvial valley floor of the Harney Basin supports wetland, riparian, and phreatophyte shrubland communities that serve as crucial habitats for a wide variety of migratory and endemic bird species in addition to many other wildlife species. As agricultural water demands in the basin have increased, so has the need to better understand the groundwater flow system and to evaluate the sustainability of water use in this region to meet diverse needs related to economic livelihoods, wildlife habitat, and recreation. The objectives of this study are to fill this knowledge gap and increase understanding of relations between variations in climate, shallow groundwater, and groundwater dependent vegetation in the Harney Basin. To accomplish this, 35 years (1984-2018) of Landsat satellite imagery, groundwater level data, and gridded climate datasets are compiled and statistically analyzed to quantify the status and trends of vegetation communities that are potentially dependent on groundwater and their relations to climate and depth to groundwater. These results were then used to guide field reconnaissance surveys, where relations were examined in greater depth.

Trend analysis results indicate widespread declines in shallow groundwater levels; in most cases these declines were determined to be occurring independently of antecedent climate conditions. In addition, substantial changes in surface water extent, vegetation vigor, and land use, indicated by the Normalized Difference Vegetation Index (NDVI), are evident over the course of the study period, with positive trends in NDVI indicating lake level declines since the mid-1980's and subsequent encroachment by sparse vegetation as well as increases in irrigated cropland. Negative trends in vegetation vigor are most prominent in mesic vegetation types and low-intensity agricultural lands used as pasture and/or hayfields. Relations are established between vegetation type, characteristic NDVI ranges, and groundwater depth ranges that can be useful for establishing benchmarks for status and trends monitoring. Site-specific analyses of field and remote sensing data identified transitions from mesic to dryland vegetation in the lacustrine fringe in response to declining lake, and possibly also groundwater, levels since the 1980's (Weaver West, Weaver, Malheur North). Other areas where trends in vegetation were evident (West Springs, Frenchglen) have limited evidence of groundwater declines and are places where non-native plant species invasions and intensive vegetation management activities such as mowing, prescribed fire, invasive plant management, and manipulation of water levels are likely influencing vegetation trends.

Understanding vegetation responses in the contexts of variable climate and groundwater is essential for quantifying current status and for monitoring past or future trends in response to changing management. The approaches described here could be readily applied to other study areas where planning objectives include consideration of sustainability of groundwater dependent ecosystems. Moreover, results from this study can be used in conjunction with groundwater model outputs to further enhance understanding of groundwater-vegetation-climate relations over space and time.

ACKNOWLEDGEMENTS

The authors wish to thank Maria Vasquez for assistance with report production and review, David Page for providing expertise in drone flight and data collection, and Ken McGwire, Mark Hausner, Laurel Saito, and Dave Decker for their reviews and suggestions

that helped to improve this report. Funding for this work was provided by the Oregon Watershed Enhancement Board, the WRG Foundation, and The Nature Conservancy in Oregon under Contract Number ORFO-090418-aa01.

CONTENTS

LIST OF ACRONYMS

AOIs	Areas of Interest
DSWE	Dynamic Surface Water Extent
EDYS	Ecological Dynamics Simulation Model
ETg	Groundwater Evapotranspiration
EVI	Enhanced Vegetation Index
GEE	Google Earth Engine
GIS	Geographic Information System
GWIS	Groundwater Information System
LaSRC	Landsat Surface Reflectance Code
LEDAPS	Landsat Ecosystem Disturbance Adaptive Processing System
NAIP	National Agriculture Imagery Program
NDVI	Normalized Difference Vegetation Index
NDWI	Normalized Difference Water Index
NHD	National Hydrography Dataset
OWRD	Oregon Water Resources Department
QA	Quality Assurance
QC	Quality Control
Rs	Solar Radiation
sUAS	Small Unmanned Aircraft System
Tdew	Dew Point Temperature
Tmax	Maximum Temperature
Tmin	Minimum Temperature
USGS	U.S. Geological Survey

LIST OF FIGURES

LIST OF TABLES

THIS PAGE INTENTIONALLY LEFT BLANK

INTRODUCTION

Situated in the northwestern Great Basin, the Harney Basin is home to a growing community of agricultural producers, in addition to the Malheur National Wildlife Refuge, one of the most important wetland complexes for migratory birds in North America (US Fish and Wildlife Service, 2013). As demands for limited water supplies have increased, so has the need to better understand the groundwater flow system and to evaluate the sustainability of water use in this region to meet diverse needs related to economic livelihoods, wildlife habitat, and recreation. To this end, the Greater Harney Valley Groundwater Area of Concern was established by the Oregon Water Resources Department (OWRD) in 2016. Related to this designation, a collaborative planning effort was initiated, and associated groundwater studies were undertaken.

Shallow groundwater beneath the alluvial valley floor of the Harney Basin supports wetland, riparian, and phreatophyte shrubland communities that serve as crucial habitats for a wide variety of migratory bird species. Yet, despite their ecological importance, little is known about how these systems have or may respond to declines in groundwater resources that have recently been observed in this region (See Appendix A for background information and review of phreatophyte responses to changing groundwater levels). The objectives of this study are to fill this knowledge gap and increase understanding of relations between variations in climate, shallow groundwater, and groundwater dependent vegetation in the Harney Basin. To accomplish this, we compiled and analyzed 35 years of Landsat satellite imagery, groundwater level data, gridded climate datasets, and field surveys for the purpose of understanding past and potential future responses of vegetation to changing climate and groundwater availability.

This study addresses the following questions:

1. What are the magnitude and direction of trends in groundwater levels in the study area?
2. How do changes in groundwater levels relate to short term (0.5-3 year) variations in climate and how do these patterns vary across the study area?
3. What are the status and trends in vegetation in the study area and how do these relate to interannual variations in climate and with depth or trends in groundwater?

We address these questions in terms of both broad characterizations of patterns across the study area and at site specific levels, focusing field investigations and in-depth analyses on areas where substantial changes have been observed over the course of the study period.

METHODS

Study Area

The study area (Figure 1) includes the alluvial valley surrounding Harney and Malheur lakes, delineated by Reed et al. (1984) as the phreatophyte boundary. The boundary roughly follows the 4200 ft MSL elevation contour and the phreatophyte zone consists of alluvium and quaternary sedimentary deposits (Smith & Roe, 2019). The area sits at the

convergence of four HUC-8 watersheds that comprise the Harney Basin: the Silvies River, Silver Creek, Donner und Blitzen, and Harney-Malheur Lakes drainages. Land ownership in the southern portion of the valley, beginning at the northern extents of the Malheur and Harney Lakes, is almost completely comprised of the Malheur National Wildlife Refuge,

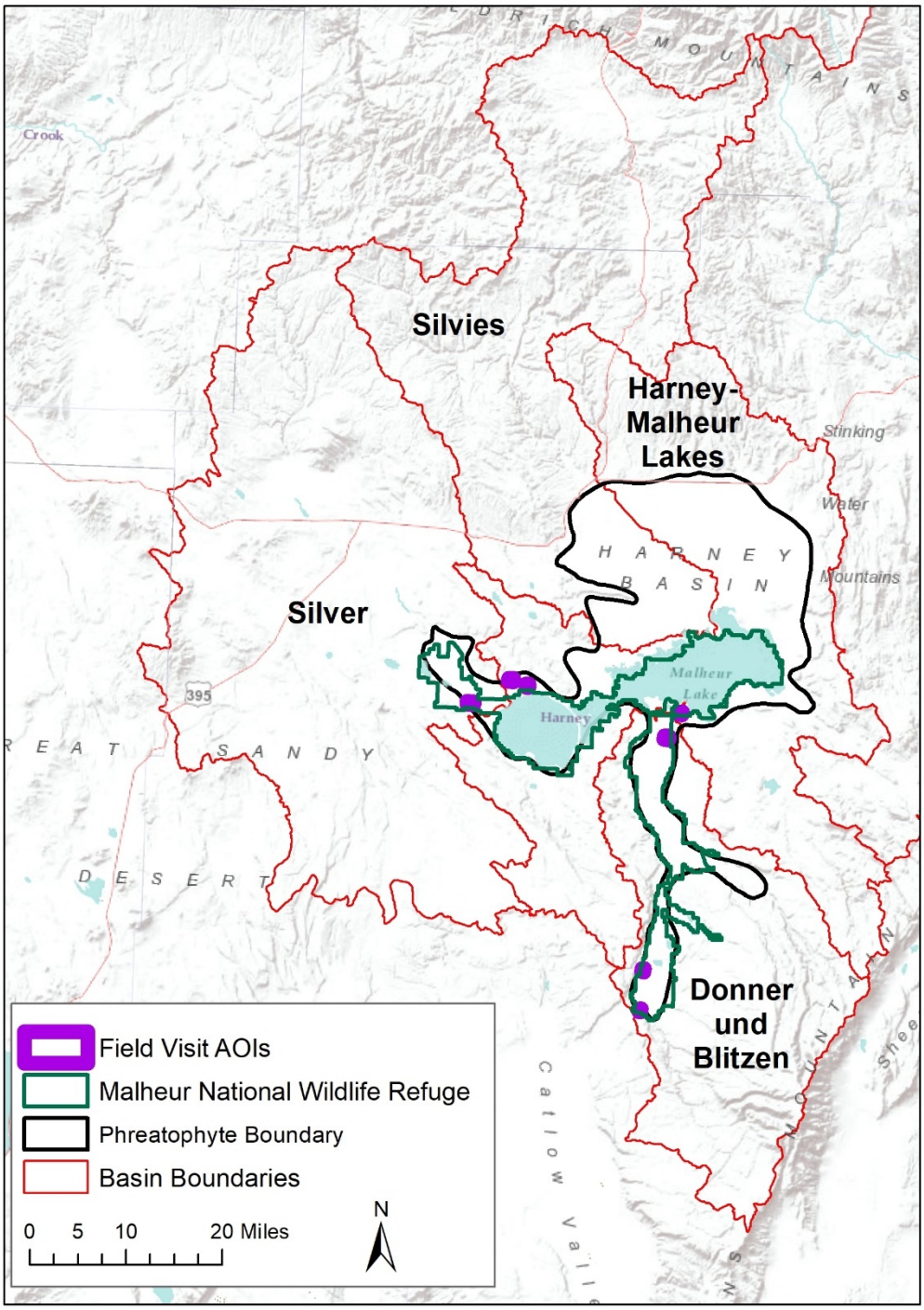

Figure 1. Harney Basin Study Area

managed by the U.S. Fish and Wildlife Service. The refuge contains a variety of lake, riverine, and wetland habitats including permanently and seasonally flooded marshes and wetlands, wet and dry meadows, and riparian woodland and shrublands that support plant species adapted to shallow groundwater conditions (US Fish and Wildlife Service, 2020). Dominant emergent plant species in freshwater marshlands include hardstem bulrush (*Scirpus acutus*), cattail (*Typha* spp.), broad-fruited burreed (*Sparganium eurycarpum*), and Baltic rush (*Juncus balticus*). Wet meadow habitats include many sedge species such as spike rush (*Eleocharis palustris*), wooly sedge (*Carex pellita*), Nebraska sedge (*Carex nebrascensis*), and slender-beaked sedge (*Carex athrostachya*), while dry meadows support herbaceous species such as inland saltgrass (*Distichlis spicata*), creeping wildrye (*Leymus triticoides*), and Nevada bluegrass (*Poa nevadensis*). Willow (*Salix sp.*) and cottonwoods (*Populus sp*.) are found in riparian woodland and shrubland habitats. Due to low relief of the terrain surrounding Malheur and Harney lakes, small fluctuations in lake water levels result in large changes in the areal extent of surface water. As such, large areas of sparsely vegetated playa habitats that are periodically inundated exist surrounding the periphery of Malheur and Harney Lakes. Wetland and sparsely vegetated areas transition to desert scrub and greasewood shrubland communities dominated by inland saltgrass and black greasewood (*Sarcobatus vermiculatus*) where alkaline soils exist, and to sagebrush shrubland and steppe communities comprised of sub-species of big sagebrush (*Artemisia tridentata*), including Wyoming sagebrush and basin big sagebrush, and rabbitbrush (*Ericameria nauseosus*) where the water table is deeper and soils are less alkaline.

Wetland and riparian habitats within the refuge are heavily managed, as surface water diversions are used extensively to control water levels within wetlands and marshes, and tools such as prescribed fire, mowing, and invasive species control are regularly used to manage vegetation to meet habitat objectives for key wildlife species (US Fish and Wildlife Service, 2013). The northern and northwestern portions of the basin are almost entirely privately owned and are predominantly managed as pasture and haylands with recent increases in areas managed for irrigated crop agriculture.

DATASETS

To address the research questions presented above, we used four existing datasets: the gridMET gridded climate dataset (Abatzoglou, 2013), the Landsat image archive available through the Google Earth Engine (GEE) cloud computing and environmental monitoring platform (Gorelick et al., 2017), the OWRD database Groundwater Information System (GWIS), and the Landfire vegetation type database (U.S. Department of Interior, 2016). These datasets were used to conduct three types of analyses, including groundwater analyses to address questions 1-2, vegetation analyses to address question 3, and site-specific analyses that used a combination of field-collected photographs, drone imagery, and qualitative observations of vegetation cover and condition to interpret status and trends for these locations.

Gridded Climate Data

The 4 km and daily resolution gridMET gridded meteorological dataset was used for all climate analyses. This dataset was selected because it is used extensively for ecological and hydrologic assessments, and it contains the variables necessary to calculate the ASCE-EWRI Standardized Penman-Monteith (ASCE-PM) reference evapotranspiration equation for a well-watered grass reference surface (Allen et al., 2005), including solar radiation (*Rs*), maximum temperature (*Tmax*), minimum temperature (*Tmin*), average dewpoint temperature (*Tdew*), and wind speed at 10 m height (*u10*). Wind speeds were logarithmically transformed to 2 m height following Allen et al. (2005) prior to calculation of reference evapotranspiration. Grass reference evapotranspiration is a measure of atmospheric water demand (Hobbins & Huntington, 2016), and is simply referred to as potential evapotranspiration in this report. For analyses of groundwater levels, the spatial average of monthly potential water surplus (precipitation minus potential evapotranspiration) was calculated for the four HUC-8 watersheds contributing to the study area (Figure 1) to represent climatic conditions across areas of potential groundwater recharge. For vegetation and site-specific analyses, potential water surplus was aggregated by water year and used at the pixel scale to reflect localized precipitation and water demand that vegetation is most likely responding to.

Landsat Archive Data

Multiple Landsat image processing steps were performed using GEE. Landsat data processing for each study area was performed largely following methods outlined in Huntington et al. (2016) and Beamer et al. (2013). The Landsat TM, ETM+, and OLI top of atmosphere reflectance was transformed to at-surface reflectance following Landsat ecosystem disturbance adaptive processing system (LEDAPS) (for TM and ETM+) and Landsat Surface Reflectance Code (LaSRC) (for OLI) atmospheric correction algorithms (Schmidt et al., 2013; U.S. Geological Survey, 2019). Landsat at-surface reflectance was used to compute the normalized difference vegetation index (NDVI) as (ρNIR - ρRed)/(ρNIR +ρRed) (Eq. 1) where ρ is the at-surface reflectance, *NIR* is near infrared waveband, and *Red* is the red waveband. NDVI was chosen over other indices because it is one of the more readily interpretable and widely used indices, does not require parameter calibration, and has been shown to perform well for quantifying vegetation cover in arid environments (McGwire et al., 2000; Wu, 2014). NDVI values for each year were calculated as the median value of clear-sky, non-cloudy images during the July 15-September 15 time period. This late summer period is optimal for assessing the relationship between vegetation vigor and interannual variability in shallow groundwater levels since precipitation and soil moisture is typically at a minimum in this region (Huntington et al., 2016). Image pixels were automatically flagged as clouds or shadows using the Fmask algorithm (Zhu & Woodcock, 2012) and were removed from the analysis. Other variables such as enhanced vegetation index (EVI), normalized difference water index (NDWI), albedo, and surface temperature were used to assist in quality assurance and quality control (QA/QC) of the NDVI time series. To adjust for changes in spectral bandwidths between sensors on Landsat 5/7 and Landsat 8, NDVI values from the latter sensor were adjusted using methods described in Huntington et al. (2016).

Oregon Groundwater Database

Groundwater level data within Harney County was obtained from the OWRD GWIS database (https://apps.wrd.state.or.us/apps/gw/gw_info/gw_info_report/Default.aspx). Groundwater level data were filtered to remove any non-static water level measurements. Only measurement data from OWRD or the U.S. Geological Survey (USGS) were included. Water level measurements are reported up to March 2019 for select wells, which marks the month at which the database was downloaded from OWRD's GWIS. Standard site information (e.g. well name, well log, measurement date range, data source, hydrograph hyperlink, latitude, longitude, etc.) is reported for each of the wells.

Landfire Existing Vegetation Type Database

The Landfire Existing Vegetation Type Database (U.S. Department of Interior, 2016) was selected to represent different vegetation communities and land uses in the study area so that comparisons in status and trends could be inferred for specific wetland, phreatophytic, and upland vegetation types. Based on visual inspection of recent high-resolution aerial imagery from the National Agriculture Imagery Program (NAIP), this dataset appeared to better distinguish natural riparian vegetation from low intensity agricultural haylands, relative to the National Land Cover Dataset (https://www.mrlc.gov/viewer/) and the National Agricultural Statistics Service croplands dataset (https://nassgeodata.gmu.edu/CropScape/). We selected 9 vegetation types based on the 'Group" level of aggregation. These included the most common natural vegetation types, including Big *Sagebrush Shrubland and Steppe, Depressional Wetland, Desert Scrub, Freshwater Marsh, Grassland and Steppe, Greasewood Shrubland, Sparse Vegetation*, and *Riparian Woodland and Shrubland* and one low intensity agricultural type - *Agricultural-Pasture and Haylands*, which comprises most of the study area. In order to keep the analysis to a reasonable number of vegetation classes and to focus on those that are most ecologically important, non-native and disturbed vegetation community types were not included in the vegetation analysis.

GROUNDWATER ANALYSES

We assessed trends in groundwater level measurements over the period of record (1984-2018) based on the non-parametric Sen's slope estimator (Sen, 1968). A minimum of 3 years of observations were required for a given well to be included in the trend analysis; 340 wells met this criterion. Although this is a small sample size, we deemed this appropriate given that it greatly increased spatial coverage of the analysis because most wells have only been measured over a few (most recent) years. An overview of data availability for the trend analysis is provided in Appendix B.

Many wells had water level measurements within the same year, therefore, the average annual depth to groundwater was computed for each year. In addition to including the standard site information, the water level database was processed and summarized per well with the following variables: number of observations (i.e. years with observations), water level minimum, maximum, standard deviation, mean, and median over the period of record, the Mann-Kendall trend test (Kendall, 1975; Mann, 1945), and Sen's slope of annual

water level rise or decline. We compared the trend test results to those based on a modified Mann-Kendall test that accounts for serial correlation (Hamed & Rao, 1998; implemented in R using 'modifiedmk' package (Patakamuri & O'Brien, 2020)) and found there to be no difference in all but two wells and thus determined that the original Mann-Kendall test provided reasonable estimates of significance. The water level summary database was joined to the GIS site database so that well locations could be attributed with water level trends and displayed on a map in combination with other geospatial datasets.

To assess the role of climate in changes in groundwater levels we conducted a partial correlation analysis (Whittaker, 1990). This allows us to isolate the associations between groundwater levels and 1) potential water surplus (indicating near-term climate variability) and 2) year (indicating a trend over time) by eliminating the effect of the other variable. A partial correlation measures the strength of the relationship between two focal variables (e.g., year and groundwater level) while accounting for the relationship of both variables to an additional variable (e.g., climate). This is accomplished by first calculating the residuals from a linear regression of each of the focal variables on the additional variable, then calculating the correlation between these residual relationships. By calculating partial correlation coefficients, we can better distinguish locations where groundwater levels are sensitive to short-term climatic variability from those that are trending over time due to other non-climate factors.

For the partial correlation analysis, we limited our analysis to wells with a minimum of 7 observations in the same quarter (Jan-Mar, Apr-Jun, Jul-Sep, Oct-Dec) to minimize the potential influence of seasonal fluctuations of groundwater levels on our results. Next, we used spatially averaged monthly values of potential water surplus (precipitation minus potential evapotranspiration) for the four contributing HUC-8 watersheds to assess correlations between annual groundwater measurements and antecedent potential water surplus aggregated at 6, 12, 18, 24, 32, and 36 months prior in order to identify the timescale that groundwater levels were most sensitive to. Once the optimal aggregation period was identified, partial correlation analyses were conducted for each well, using year and the optimal potential water surplus aggregation value as predictors and groundwater level for a given quarter as the response. Prior to finalizing results, data from each well were evaluated to ensure that assumptions of normality (indicated by skewness and kurtosis) and homogeneity of variance were met and that influential outliers were removed (determined as values > 4 times the mean Cook's distance). Statistical analyses were performed in R; tests of regression assumptions were completed using the gvlma function in the 'gvlma' package (Peña & Slate, 2006) and partial correlation analysis was performed using the pcor.test function in the 'ppcor' package (Kim, 2015). An overview of data availability for the partial correlation analysis is provided in Appendix B.

VEGETATION TREND ANALYSES

We assessed trends in annual late summer (median July 15-September 15) NDVI over the 1984-2018 time period on a per-pixel basis using the non-parametric Sen's slope estimator (Sen, 1968). In addition to the trend analysis based on annual NDVI values, climate-adjusted trends in NDVI that account for influences of potential water surplus on

NDVI were calculated using the Adjusted Kendall approach described in Alley (1988) and Section 12.3 in Helsel & Hirsch (2002). Potential water surplus was calculated for each water year and an ordinary least-squares linear regression analysis between potential water surplus and NDVI values was conducted for each pixel. From there, Sen's slope estimations were conducted on the regression residuals (observed NDVI minus predicted NDVI) for each pixel. All NDVI trend analyses were conducted in the GEE cloud computing environment. We limit our inferences to interpretations of the Sen's slope estimator in part because our primary intention is to describe the direction and magnitude of trends as opposed to determining 'significance' based on an arbitrary threshold. In addition, we observed one-year lagged temporal autocorrelations of varying strength across the study area, which can make p-values calculated from the Mann-Kendall trend test unreliable. Because a modified Mann-Kendall test that accounts for temporal autocorrelation is currently not functional in GEE, and because we did not view 'significance' as critical to the interpretation of our results, improved measures of statistical significance (e.g., through a modified Mann Kendall test) were not pursued further but will be in the future.

VEGETATION STATUS ANALYSES

To assess changes specific to key ecosystem types within the study area, we assessed the status and trends of NDVI within individual vegetation types identified based on the Landfire dataset described above. For Landsat pixels overlapping pixels of each vegetation type, we characterized the range of trend slope directions and magnitudes that occurred. We further characterized the historic ranges of NDVI values across the study area by calculating decadal average NDVI for each pixel for the periods 1990-1999, 2000-2009, and 2010-2019. Ranges of NDVI values for each vegetation type and decade were plotted as boxplots and differences were qualitatively compared to understand the magnitude and direction of changes that have occurred over time. Finally, we compared contemporary (2010-2019) ranges of NDVI values common to each vegetation type as a foundation for understanding future changes in these systems.

VEGETATION RELATIONS TO GROUNDWATER ANALYSES

To gain insights into the ranges of shallow groundwater depths associated with each vegetation type, a map of estimated water table depths for the phreatophyte zone for winter/spring 2018 was generated. This time was selected based on the availability of ~ 230 groundwater level measurements for the January-March time period from a large synoptic sampling effort by USGS and OWRD. The estimated water table depth map was based on three data types. The first type was groundwater depth measurements for shallow groundwater wells (defined as those with open interval start depths < 75 ft and end depths < 200 ft) that were collected during January-March 2018 synoptic study. The second was satellite observations of surface water presence using the Landsat Collection 1 Level 3 Dynamic Surface Water Extent (DSWE) product (U.S. Geological Survey, 2018) for the time period closest to that of the groundwater observations. Images from April 23, 2018 were used, as these provided the best images that were unobstructed by snow and cloud shadows. The third was a map of perennial water features, including perennial lakes/ponds, reservoirs,

and swamp/marshes based on the National Hydrologic Dataset Plus. The DSWE data were used to complement the NHD perennial water features dataset, as this former dataset captured ephemeral/ intermittent water features present during the time of the groundwater study. Polygons representing surface water extents from the DSWE dataset were merged with the NHD perennial features dataset in ArcGIS and points were created at 10 km intervals along the polylines of these features. Land surface elevation values were then extracted at each point based on a 30 m resolution digital elevation model to represent the elevation of the water surface. Similarly, land surface elevation values were extracted for each well point location (n=35) and depth to water measurements were subtracted from these to derive the elevation of the water table at these locations. Points representing water surface elevations (n=210) based on the surface water features and wells datasets were then merged together and used to generate an interpolated map of water table surface elevations that could be linked with vegetation. This was accomplished using a 2nd-order local polynomial interpolation with an exponential kernel smoothing function in ArcGIS Geostatistical Analyst. The model optimization parameter was selected, which varies numerous model parameters to generate a best-fit model. Prediction and standard error surfaces were masked to the phreatophyte boundary and used for inference. Cross validation of the interpolated water table surface for Winter/Spring 2018 showed reasonable model fit with the data, with mean error of 0.323 ft and a RMSE of 8.09 ft, but a slight bias toward predicted water table depths that are shallower (higher elevation) relative to observed (Figure 2). As a final step, the water surface elevation layer was subtracted from the land surface elevation to generate a depth to water surface.

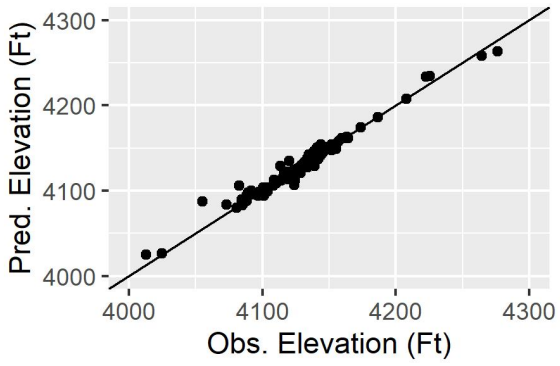

Records	210
Method	**Local Polynomial Interpolation**
Kernel function	Exponential
Output type	Prediction
Power	2
Bandwidth	13,793.233746190066
Spatial condition number threshold	347.7104987598
Exploratory trend surface analysis	52
Searching neighborhood	Standard
Neighbors to include	1,000
Sector type	Full
Major semiaxis	17,241.542182737583
Minor semiaxis	17,241.542182737583
Angle	0

Figure 2. Model parameters and cross validation results for interpolated water table surface.

SITE-SPECIFIC ANALYSES

Detailed analyses and field visits were conducted for seven areas of interest (AOIs) within the study area where previously described groundwater and vegetation analyses indicated trends in NDVI and groundwater levels. Land ownership, road access, and travel distances were all considerations in selecting the field sites. Because the northern part of the study area is nearly all private land, field sites were limited to the central and southern parts, both of which are within the refuge. Field visits to each site were conducted on August 26-27, 2019.

Once at each site, we established one or more transects of approximately 100 m. Five photographs were taken (one in each of the cardinal directions and one facing the ground) at each of four points (0 m, 25 m, 75 m, 100 m) along the transect. Coarse-level estimates of percent cover were made for greasewood, rabbitbrush, riparian trees (cottonwood, willow, wood's rose), bulrush-cattail marsh, graminoids, non-native tree species, non-native noxious species, other species that may affect the greenness signal, open water, bare ground, and cow pies within 5 m on either side of the transect were made. A qualitative ranking of water stress was applied to the first four categories based on stem mortality (< 15% stem mortality =low, 15-49% = intermediate, > 49% = high). Additional site observations documenting disturbance or stress were also recorded. Records were then input into a GIS database and were attributed with information corresponding to the site photographs provided in the database.

Small unmanned aircraft system (sUAS) flight operations were also conducted above each of the 100 m transects using a DJI Phantom 4 Pro. Flights were performed at heights of roughly 30 m above ground level. Flights were pre-programmed using the Maps Made Easy application for IOS. Visible (red, green, and blue: RGB) and false color (red, green, and near-infrared: RGN) snapshots were taken every second during the sUAS flights. A stock CMOS camera was used to collect the visible imagery, whereas a Survey3 MapIR camera was used to collect false color imagery. A 12.5 x 10.0 x 1.25 in. ground calibration target was used to gather reference spectra during each of the flights in order to calibrate the false color images during post-processing. The calibration target was composed of four different colored felt-like squares (black, dark gray, light gray, and white), each with known reflectance curves. False-color images were pre-processed and calibrated using the MapIR camera control software (https://www.mapir.camera/collections/software). Visible and false color images were then analyzed and stitched into high-resolution (<2 cm pixel resolution) orthomosaics using the Agisoft Metashape Professional software. Orthomosaics were then georeferenced within a geographic information system (GIS) using ESRI ArcMap 10.7. Stitched false color images were then used to compute a normalized difference vegetation index (NDVI).

For each AOI and transect, spatial averages of annual gridded climate, NDVI, and other selected vegetation index values were calculated and analyzed to provide a more detailed view of interannual variability and long-term change than could be provided by the long-term linear trend analyses conducted for the entire study region. Selected hydrographs for wells near Area of Interest field sites are included in Appendix C.

RESULTS AND DISCUSSION

CLIMATE TRENDS

Variability and trends in climatic conditions in the basins contributing to the study area provide important context for interpreting changes in groundwater and vegetation condition. Spatially averaged water year (Oct-Sept) precipitation, potential evapotranspiration, and potential water surplus (precipitation minus potential evapotranspiration) for the Silvies, Silver, Donner und Blitzen, and Harney-Malheur Lakes

HUC-8 watersheds are shown in Figure 3. While interannual variability in these variables exists, there was no significant trend in these conditions over the course of the 1984-2018 time period (Figure 3). This result suggests that any linear trends in groundwater or NDVI for the 1984-2018 time period are unlikely to be strongly affected by climate.

GROUNDWATER ANALYSES

It is important to note that groundwater trends for individual wells vary in the time period, seasonal timing, and consistency of measurements (See Appendix B for overview of groundwater level data availability) and these may all strongly affect resultant trend slopes. Wells with a minimum of 3 years of groundwater depth observations during 1984-2018 (n = 340) were included in the trend analysis. Negative trends in well depths to groundwater were evident at most locations, based on Sen's slope results (Figure 4). In most cases, declines in water levels are on the order of a few feet per year, but some areas are exhibiting much larger trends in either direction, especially the Weaver Springs area and the northeast portion of the phreatophyte zone.

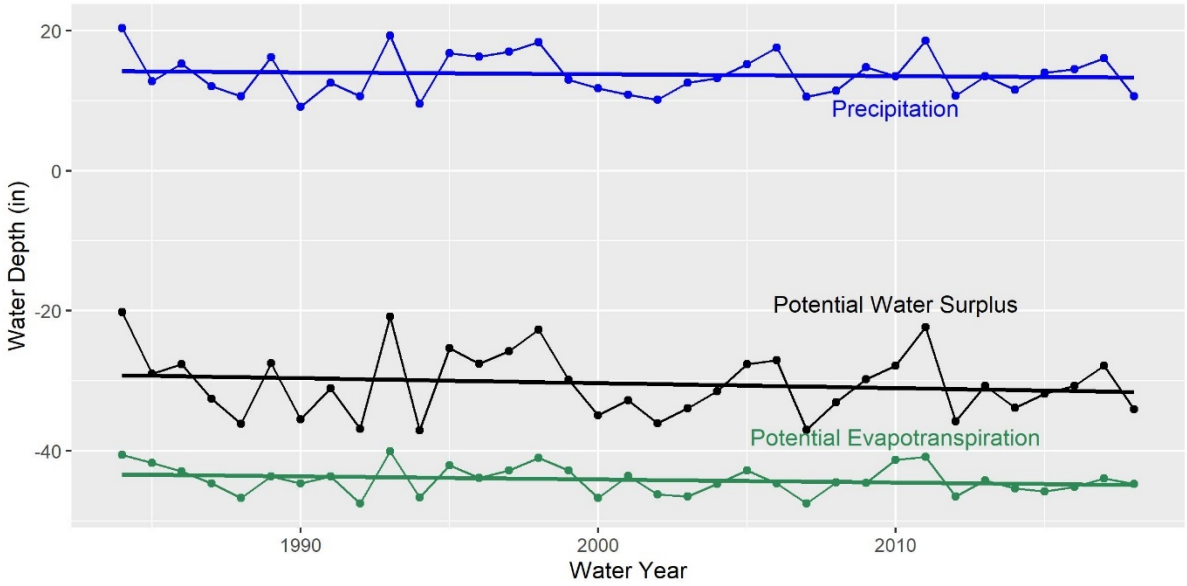

Figure 3. Variability and trend in water year precipitation, potential evapotranspiration (shown as a negative value), and water surplus (precipitation minus potential evapotranspiration) averaged over the Silvies, Silver, Donner und Blitzen, and Harney-Malheur Lakes (HUC-8) watersheds for the 1984-2018 study period. Data are fit with least-squares regression line to show overall directions of trends over time for each variable, which were not significantly different from zero (p =0.50, 0.25, and 0.34 for precipitation, potential evapotranspiration, and water surplus, respectively).

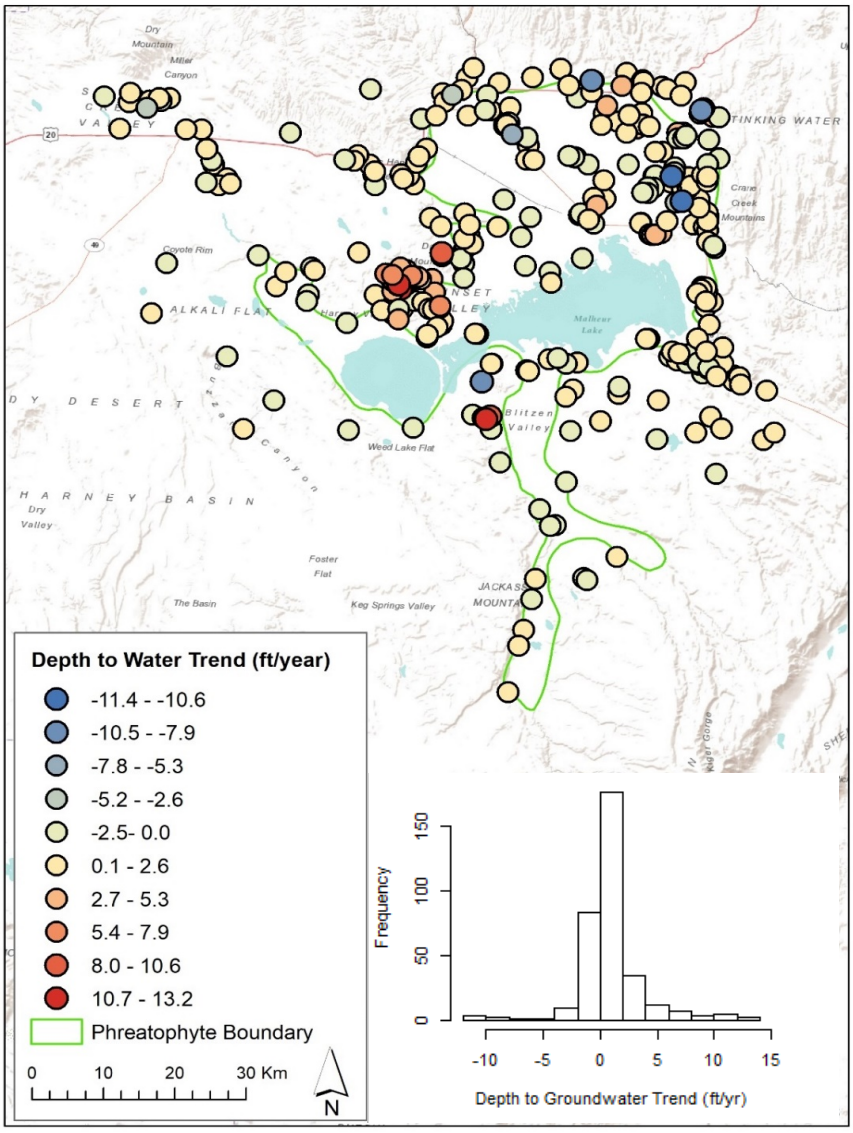

Figure 4. Sen's slope trend calculations for 340 groundwater wells with a minimum of 3 years of observations. Positive values (red) indicate increased depth to groundwater over time (lowered groundwater levels).

Wells with a minimum of 7 observations (n=68) within a single quarter during 1984-2018 (see Appendix B for overview of data availability) were included in the partial correlation analysis. Partial correlation coefficients between groundwater depth (ft) and time (year; an indicator of trend and surrogate for factors that are driving the trend), after accounting for the relationship with potential water surplus, were greater than 0.6 for 80 percent of the wells, suggesting declines are strongly associated with factors other than near-term (6 to 36 month) antecedent climate. With one exception, weaker correlations with year only occurred for wells with maximum measured depths less than 60 ft (Figure 5), indicating that some wells with shallower water levels were not trending as strongly over time. This result generally fits with expectations, as shallower groundwater is more likely to

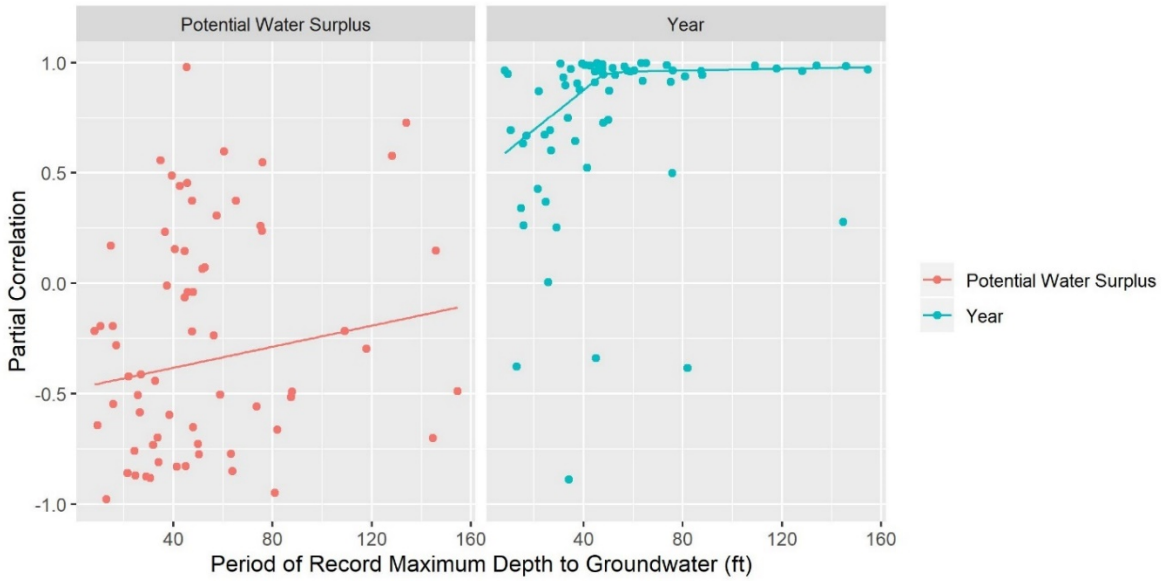

Figure 5. Partial correlations between depth to groundwater and potential water surplus (precipitation minus evapotranspiration; left) and year (right) plotted against period of record maximum depth to groundwater. Partial correlations closest to -1 for potential water surplus indicate wells at which groundwater levels decline under drier climatic conditions and thus have high sensitivity to short-term fluctuations in climate. Partial correlations closest to 1 for Year indicate increasing depth to groundwater over time. A median-based spline smoother is fit to the data to highlight relations between partial correlations and maximum recorded depth to groundwater. Wells with shallower depths tend to have greater sensitivity to climate, while wells with deeper depths tend to be less sensitive to climate and exhibit more consistent (declining) trends over time.

have shorter flow paths, more local recharge areas, and less variability in source area and travel time while deeper groundwater is likely to be fed by a larger catchment area and have more variability in recharge area and travel time, thus smearing the climate response.

Partial Correlations between groundwater depths and potential water surplus were less consistently strong. The expected correlation between depth to groundwater and potential water surplus is negative, as drier years are expected to have deeper groundwater depths. About 30 percent of the wells have negative correlations less than -0.6 (Figure 5), indicating that these had relatively strong relations with climate, after accounting for the relationship with year (i.e., after accounting for trends over time). Stronger negative correlations tended to be more prevalent in wells with shallower depths to groundwater (Figure 5). Correlations between potential water surplus and groundwater depth tended to be highest in the northern part of the study area where mountain front recharge is likely to be most influential (Figure 6a). Relations between year and groundwater depth were strong in many parts of the study area (Figure 6b), suggesting a substantial role of factors other than near-term climate as drivers of declining groundwater levels. The integrated timescale (0-6 to 0-36 months previous) of antecedent potential water surplus that was most highly correlated with groundwater levels varied among wells with no discernable pattern; most wells were correlated at either the 12- or 36-month timescale (Figure 6c).

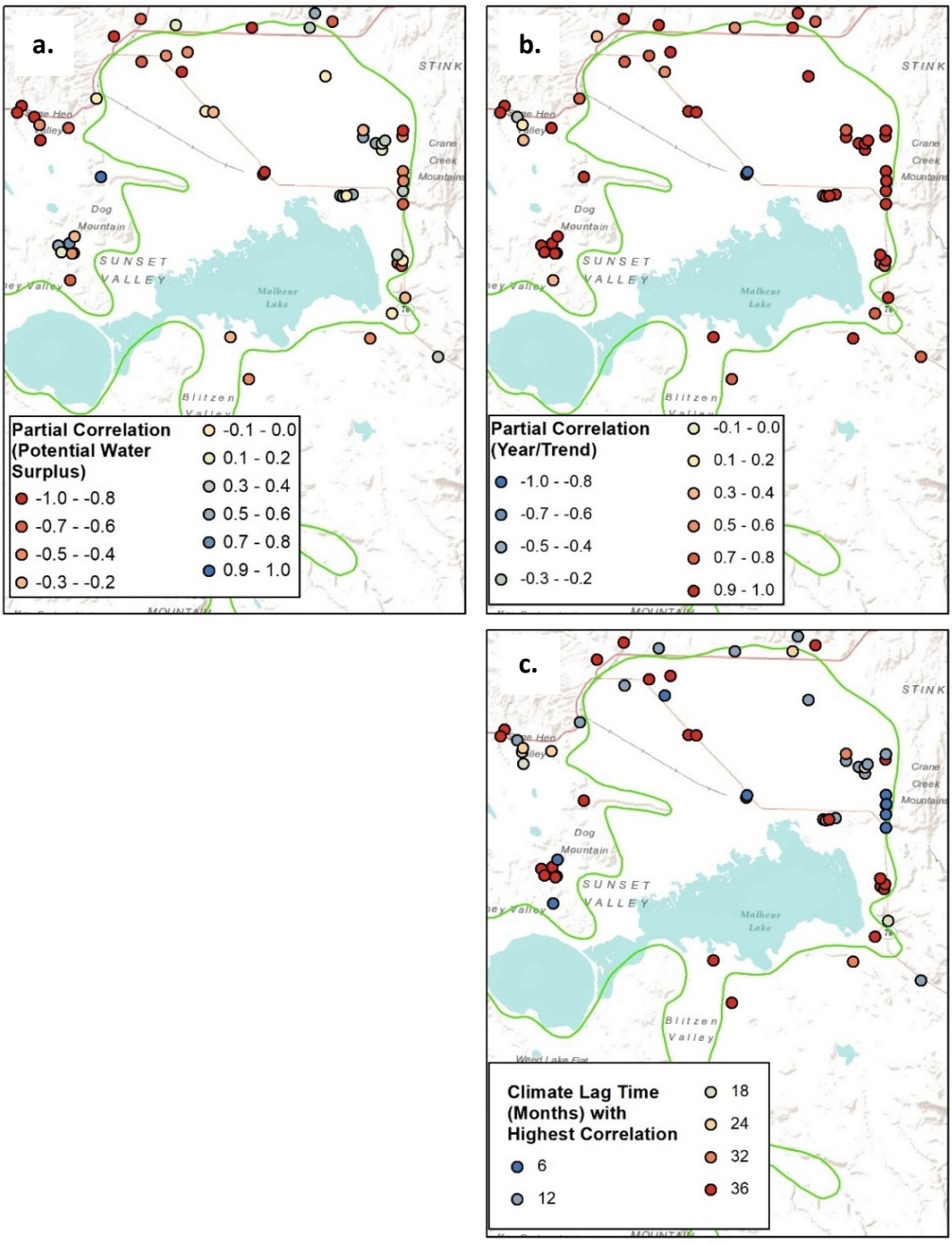

Figure 6. Partial correlations between depth to groundwater and a) potential water surplus (precipitation minus evapotranspiration) and b) year. Partial correlations closest to -1 (red) for potential water surplus indicate wells at which groundwater levels decline under drier climatic conditions and thus have high sensitivity to short-term fluctuations in climate. Partial correlations closest to 1 (red) for Year indicate trends of increasing depth to groundwater over time. c) shows the timescale of antecedent potential water surplus that was most highly correlated with groundwater levels that was used in the partial correlation analysis.

VEGETATION TREND ANALYSES

A wide range of trends can be observed within and surrounding the study area (Figure 7). Blue areas, indicating increases in greenness are commonly observed in irrigated agricultural fields, within surface water bodies (due to increased turbidity), and within playa areas of Harney and Malheur Lake. In these latter cases, increasing NDVI signifies declines in surface water (standing water has negative NDVI values). Differences between the raw and climate-adjusted trends are minimal, which is to be expected given that there was little trend in climate over the course of the study period. By reducing the noise caused by interannual climate variability, the climate adjustment resulted in steeper trend slopes in some cases (indicated by darker colors).

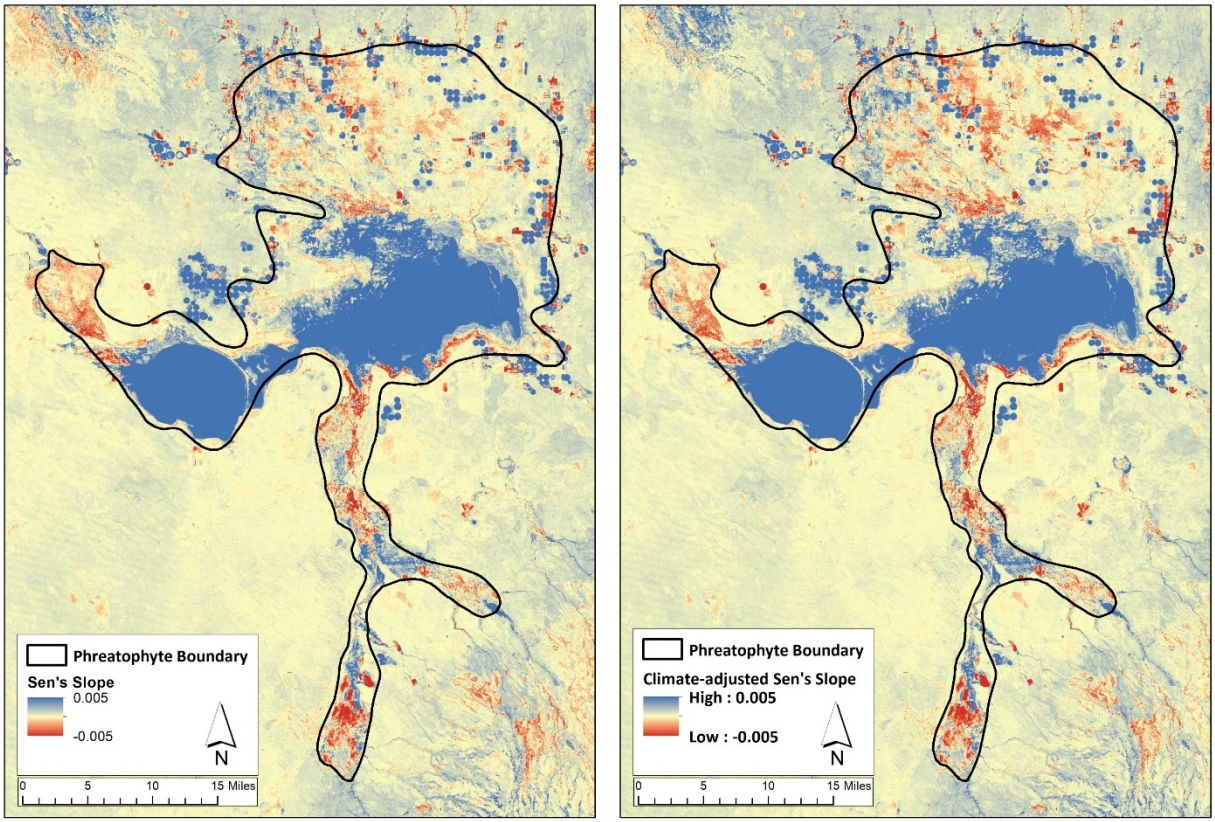

Figure 7. Trends in late summer (July-Sept) NDVI from 1984-2018 based on Sen's slope estimator for raw NDVI values (left) and following adjustment for interannual climate variability (right).

Differences in climate-adjusted trends among key vegetation types (Figure 8) within the study area are evident (Figure 9). In particular, the *Sparse Vegetation* type that extends across the Harney Lake playa and around the periphery of Malheur Lake shows the most obvious change, with over 90 percent of pixels exhibiting positive NDVI trends, as this area was covered in water at the start of the study period and has since dried and been colonized by sparse vegetation. Surface water declines are indicated as positive trends in NDVI because surface water has lower NDVI than bare ground or vegetation. Differences among other

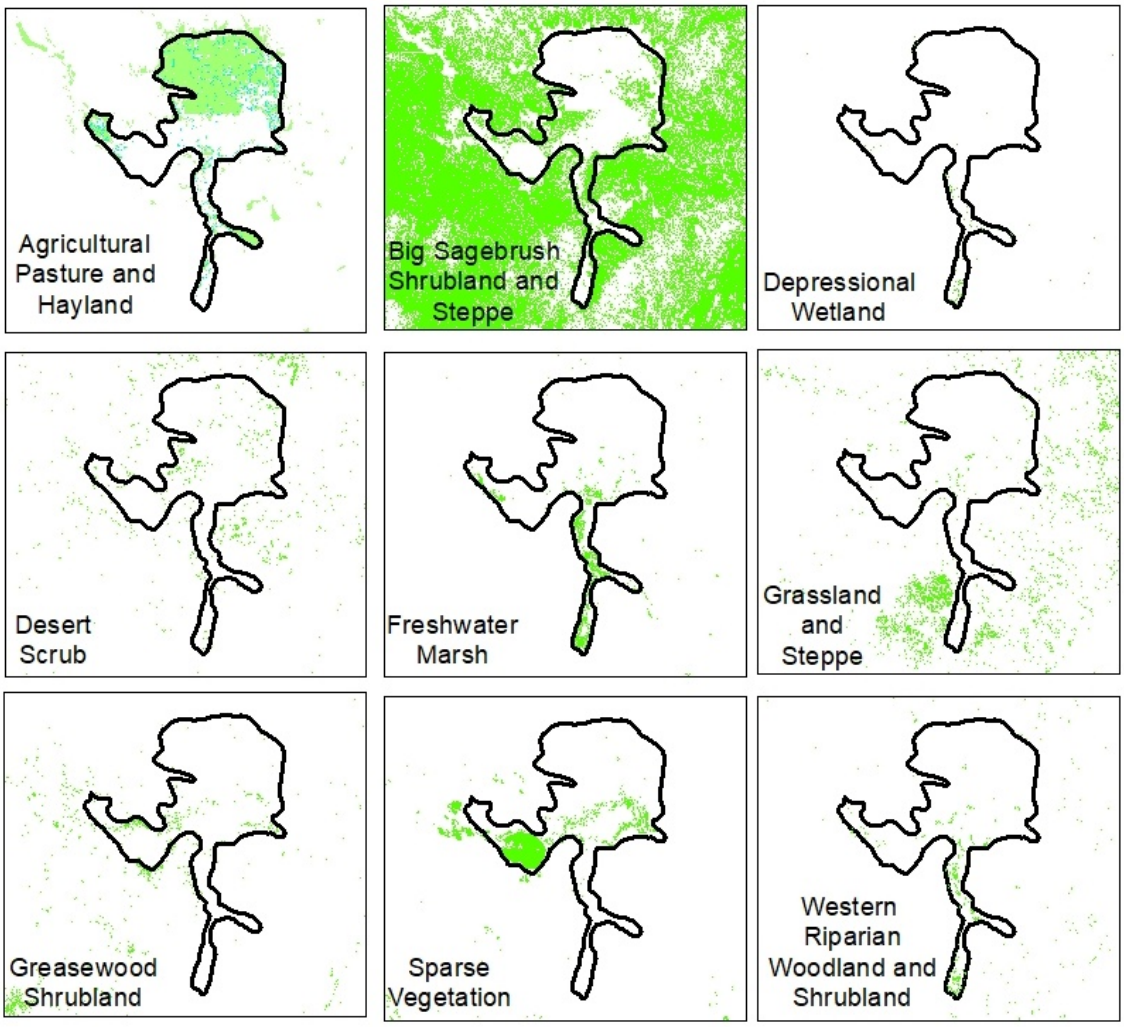

Figure 8. Locations of nine focal ecosystems within the Harney Basin phreatophyte zone (green line).

vegetation types are more subtle. For most other types, approximately 50-75 percent of pixels had positive trends (Figure 9). Part of the reason for large proportions of positively trending pixels is explained by Figure 10, where pixels with negative NDVI values indicate the presence of water during the 1990-1999 time period that is no longer present in later decades. Pixels with negative NDVI values during 1990-1999 are present within every vegetation type. These pixels are places where substantial change and vegetation type conversion may have occurred with declining water availability. For example, standing water was clearly present and persistent over the 1990-1999 decade in many areas that are now classified as dryland shrubland, grassland, and scrubland vegetation types (Figure 7). Except for the *Sparse Vegetation* type, approximately 25-50 percent of pixels for each ecosystem type had negative trends. *Riparian Woodland and Shrubland*, *Depressional Wetland*, *Freshwater Marsh*, and *Agricultural Pasture and Hayland* had the largest proportions of negative trends, but at the decadal scale and when all pixels of a given vegetation types are lumped together, none of these vegetation types exhibit substantial shifts in NDVI across decades (Figure 10).

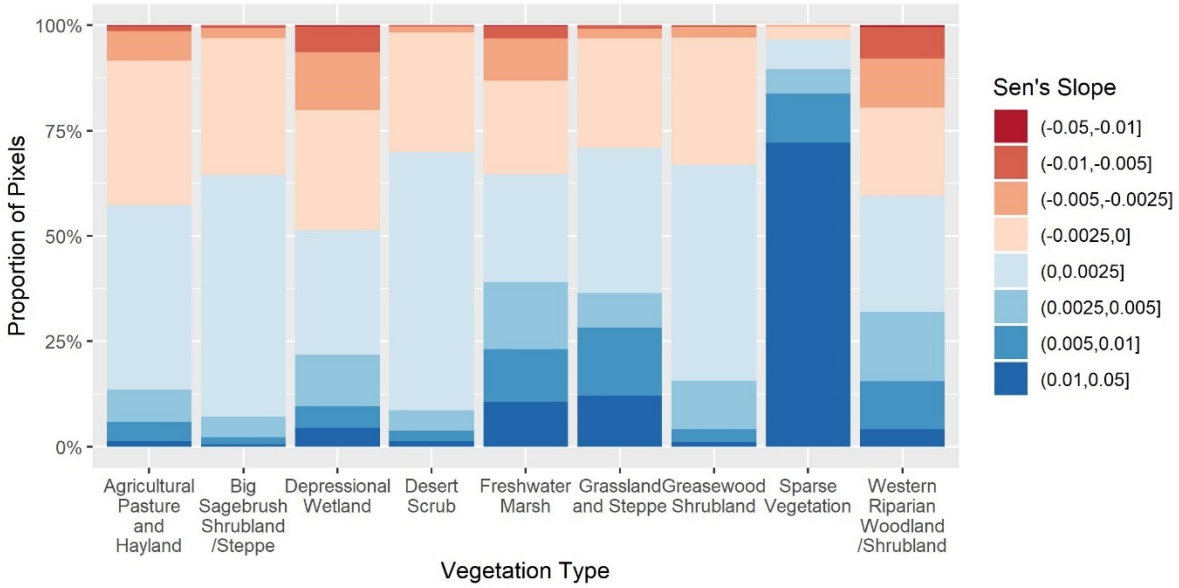

Figure 9. Proportions of pixels with varying positive and negative trend slope magnitudes in climate-adjusted NDVI from 1984-2018.

VEGETATION STATUS ANALYSES

Understanding the ranges of NDVI values that are typical for different ecosystem types provides an important basis for understanding and monitoring the status and trends in vegetation using satellite remote sensing data. Such information can help to identify locations that are potentially in transition and the point at which such transitions might be interpreted as meaningful ecological change. For example, pixels with particularly high or low NDVI values compared to others within the same ecosystem type might signify places of disturbance, vegetation type change, edge effects, or possibly misclassification. Figure 11 and Table 1 illustrate the observed ranges of NDVI values for each vegetation type based on average NDVI for each pixel over the 2010-2019 time period. Obligate groundwater ecosystem types such as *Depressional Wetland*, *Freshwater Marsh*, and *Western Riparian Woodland and Shrubland* have clearly higher ranges of NDVI values relative to other vegetation types, with an NDVI value of 0.3 separating all wetland types from those that may be less groundwater dependent (with the exception of *Agricultural Pasture and Haylands*, also contain mesic vegetation due to irrigation). NDVI values of 0.4 and 0.2 may serve as additional thresholds for signifying wetland and sparsely vegetated ecosystem types, accordingly in this study area.

Using the threshold of 0.3 for defining mesic/wetland areas, we assessed transitions in mesic vegetation and surface water from the 1990's to the 2010's based on 10-year average NDVI values. Mesic vegetation losses (gains) were attributed to those pixels with a 10-year average NDVI greater (less) than 0.3 for the 1990-1999 time period and a 10-year average NDVI less (greater) than 0.3 for the 2010-2019 time period. Surface water losses were

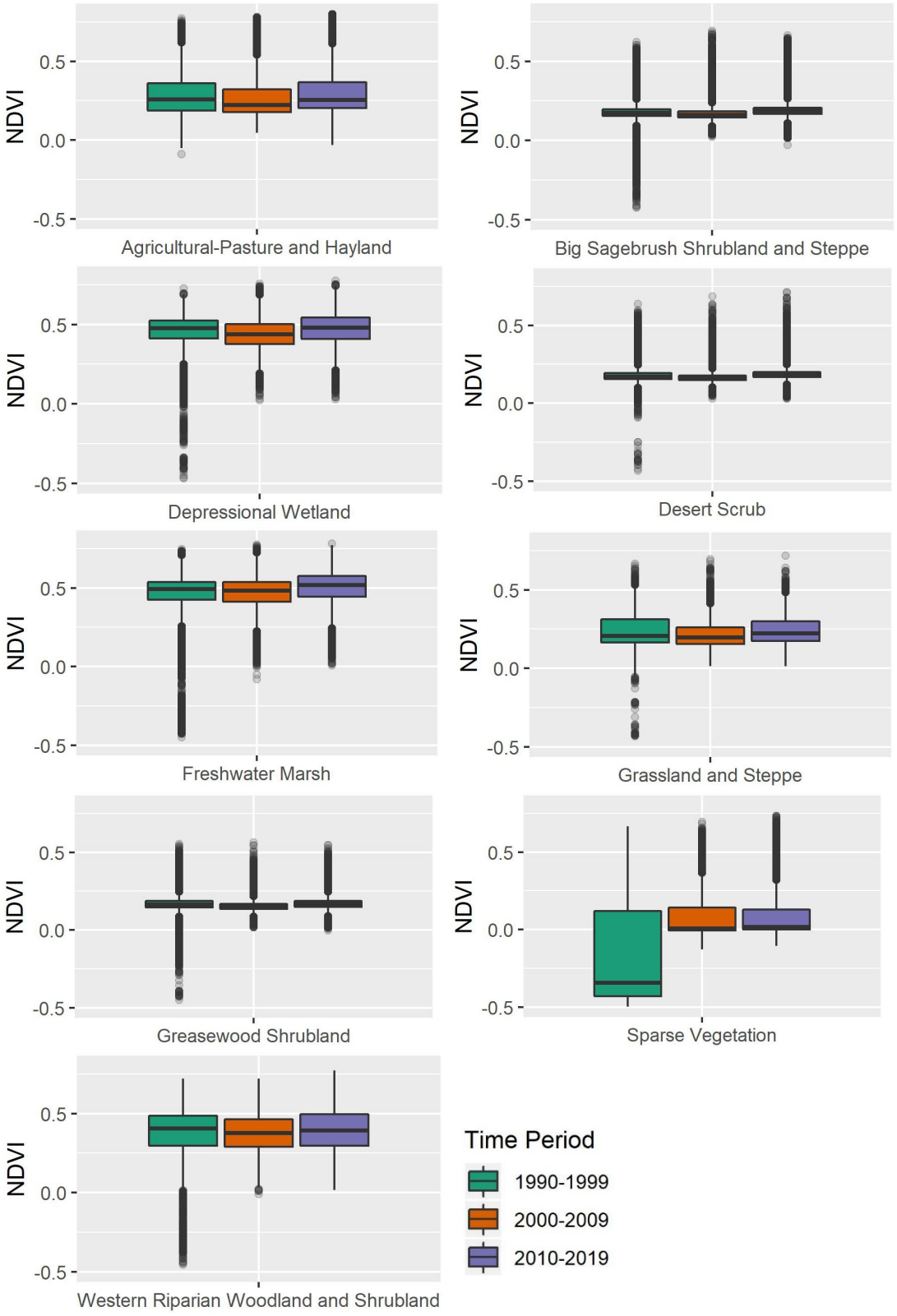

Figure 10. Distributions of decadal average NDVI values for nine focal ecosystem types for 1990-1999, 2000-2009, and 2010-2019 periods. NDVI values < 0 indicate the presence of surface water.

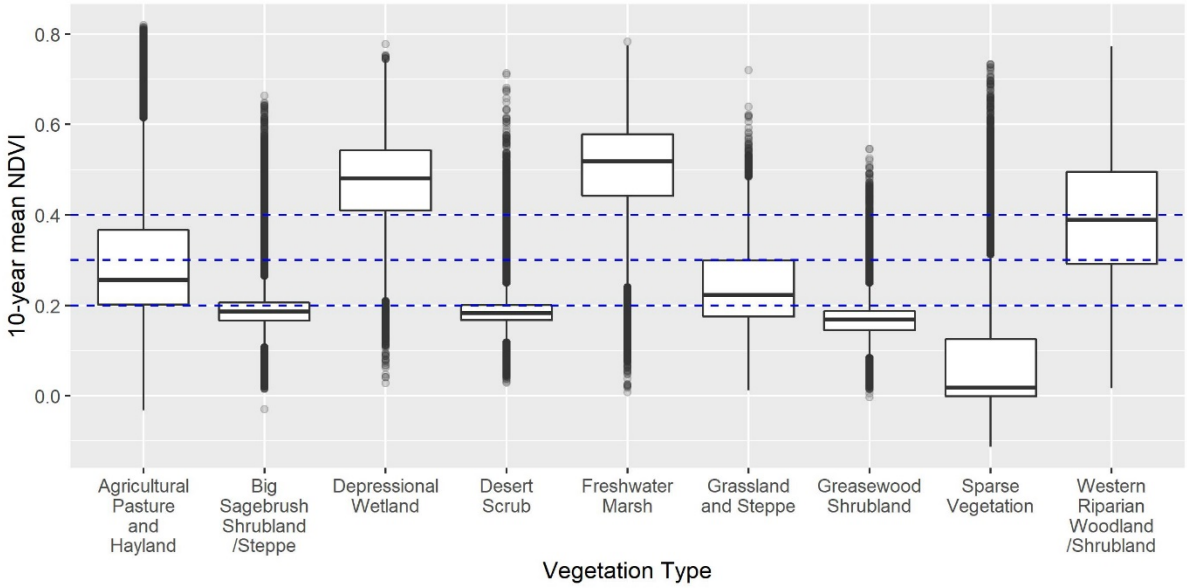

Figure 11. Contemporary ranges of NDVI values (10-year mean 2010-2019) for key ecological systems in the Harney phreatophyte zone. Riparian and wetland vegetation types typically have NDVI values > 0.3 and 0.4, respectively, while dryland vegetation types typically have values between 0 and 0.2.

Table 1. Typical ranges of late-summer NDVI values for focal vegetation types in the Harney Basin phreatophyte zone.

	Range of NDVI Values		
Vegetation Type	**25th Percentile**	**Median**	**75th Percentile**
Agricultural Pasture and Hayland	0.2	0.26	0.37
Big Sagebrush Shrubland /Steppe	0.17	0.19	0.21
Depressional Wetland	0.41	0.48	0.54
Desert Scrub	0.17	0.18	0.2
Freshwater Marsh	0.44	0.52	0.58
Grassland and Steppe	0.18	0.22	0.3
Greasewood Shrubland	0.15	0.17	0.19
Sparse Vegetation	0	0.02	0.13
Western Riparian Woodland/Shrubland	0.3	0.39	0.5

attributed to those pixels with 10-year average NDVI less than zero for the 1990-1999 time period and greater than zero for the 2010-2019 time period (Figure 11). Based on these results, an estimated 631 acres of mesic vegetation losses occurred between these two time periods. The majority (69%) of these acres are, as of 2016, classified as *Agricultural Pasture and Haylands*; however, it is unclear whether these losses are a function of wetland/mesic conversion to pasture/hayland or if this represents changes in management (e.g., timing of fallow and flood irrigation schedules that result in drier late summer conditions) or species composition in pasture/haylands that have been in use for multiple decades. Although mesic pasture/haylands do not provide the same wildlife value as natural mesic vegetation types, they remain highly important in areas where losses of natural wetlands have occurred (Donnelly et al., 2016). The other 31% of mesic losses mostly occurred on lands classified (as of 2016) as *Big Sagebrush Shrubland and Steppe, Introduced Perennial Grassland and Forbland, Sparse Vegetation, Freshwater Marsh, and Western Riparian Woodland and Shrubland.* Mesic vegetation gains occurred over 892 acres based on this method. Notably, most of these gains occurred on agricultural lands (37% on pasture/haylands and 41% on other irrigated agricultural crop types), with only 82 acres of these gains occurring in pixels classified as natural (undisturbed, undeveloped, native species dominated) communities. Places where large areas of mesic vegetation transition to lower NDVI values include in the Warm Springs Valley, the southern periphery of Malheur Lake, and in the vicinity of Poison Creek and Ninemile Sloughs in the northern part of the study area (Figure 12).

VEGETATION RELATIONS TO GROUNDWATER

The water table depth surface presented here represents a very coarse, first-approximation of water table depths (Figure 13). Due to the simplicity of the interpolation algorithm, results should be interpreted with caution, especially around the periphery of the study area, where fewer points were available to fit the model and where discontinuities in land surface elevation or steep land surface elevation gradients have the potential to result in large error with water table estimates that are well above or below the land surface. In addition, the cross-validation results (Figure 2) and mapped surface (Figure 13) indicate a bias toward shallower depths in the result. Water table surface estimates may be improved as more information becomes available, with the application of more sophisticated interpolation methods and manual delineation, and with carefully informed selection of shallow wells and surface water features representative of the natural water table surface. In the meantime, we demonstrate the application of estimated groundwater depths to gain initial insights into associations between water table depth and key ecological system types within the study area. Because the estimated water table surface represents winter/early spring conditions, it is expected that these values are representative of annual minima water table depths (i.e., seasonal high water table) as opposed to depths represented by end-of-growing season conditions, which may be up to several feet lower and is more likely to control the distributions of wetland-obligate species.

As may be expected, wetland, marsh, and riparian vegetation types were associated with narrow interquartile ranges of shallow water table depths between 2 ft above and 4 ft below the land surface (Figure 14, Table 2). With a few exceptions, these vegetation types are limited to the phreatophyte zone (Figure 7). While no information on groundwater depths

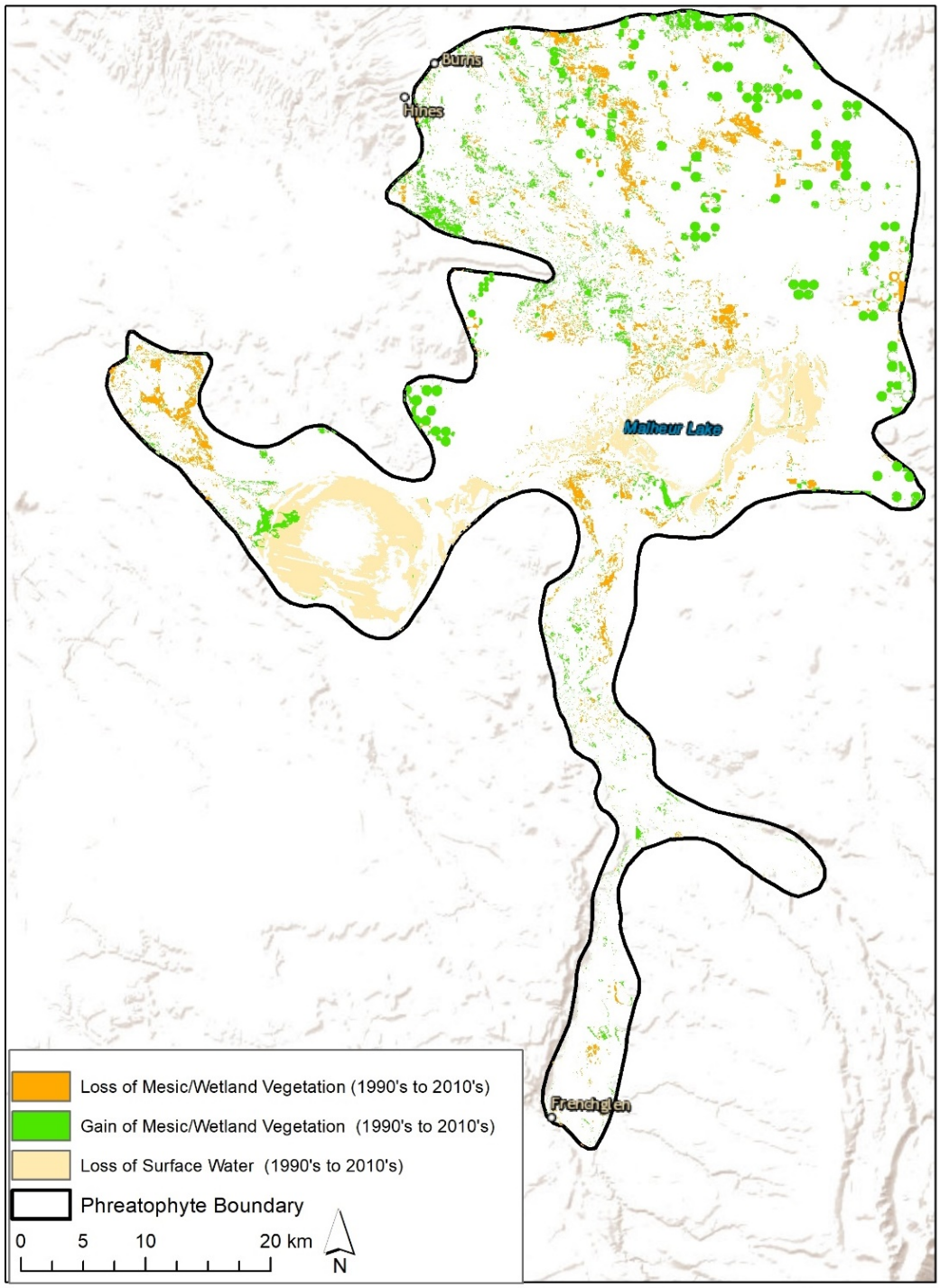

Figure 12. Gains and losses in mesic and wetland vegetation types based on changes in 10-year average late-summer NDVI between the 1990-1999 and 2010-2019 time periods across a threshold NDVI value of 0.3, indicating mesic vegetation communities (see Figure 10). Losses in surface water over these same time periods are based on changes in NDVI from < 0 to > 0 between the two decades.

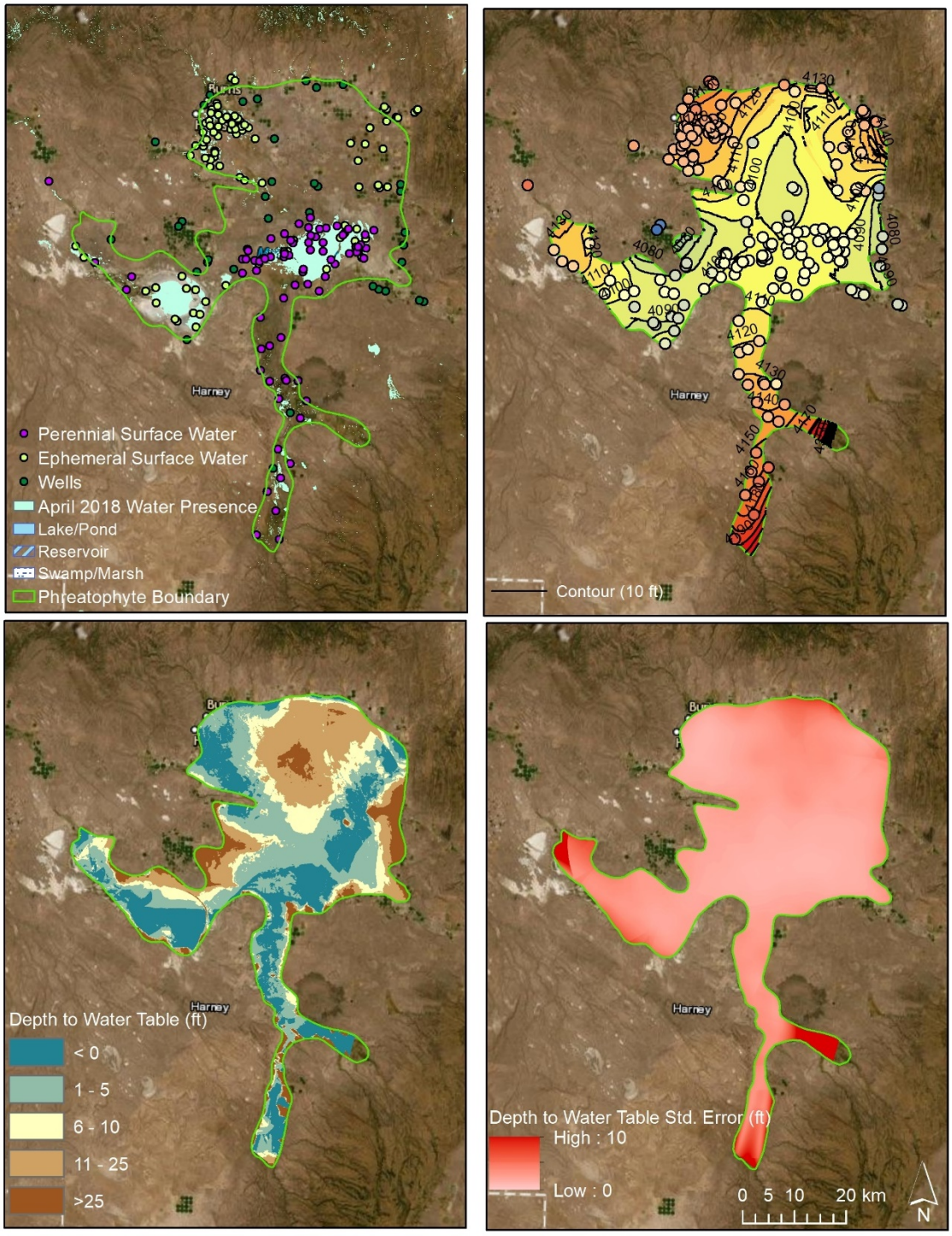

Figure 13. Input points used to generate the interpolated water table elevation surface (upper left), the resultant interpolated water table elevation surface (upper right), depth to water table (i.e., the difference between water table elevation and land surface elevation; lower left), and the standard error surface generated from the 2nd order Local Polynomial Regression algorithm implemented in ArcGIS.

are available for woody riparian vegetation types, estimated interquartile ranges of groundwater depths (Table 2) are generally within the range of those reported for other wetland types within the Malheur National Wildlife Refuge. *Emergent Marsh* water depths in the Malheur NWR typically range from 2-3 inches to 2-3 ft above the land surface but may recede below the land surface in dry years (Christy, 2016), *Seasonally Wet Meadows* range from sub-irrigated to 1 ft in depth, and *Seasonally Flooded Marshes* range from 3 feet above to 4-5 inches below the soil surface (US Fish and Wildlife Service, 2020). Sparsely vegetated areas comprised mostly of the Harney Lake playa and areas around the periphery exhibited a similar range, with water table depths of up to 5 ft. Greasewood shrublands and desert scrub within the phreatophyte zone occurred over a larger range of groundwater depths between 3 and 17 feet below the land surface (Figure 14, Table 2), consistent with typically observed ranges reported in the literature for greasewood (Nichols, 1994; Robinson, 1958). The two other dryland vegetation types, *Big Sagebrush Shrubland and Steppe* and *Grassland and Steppe*, which are not expected to be groundwater dependent, occurred in association with deeper and wider ranges of groundwater depths and were also common outside the phreatophyte zone (Figure 7).

SITE-SPECIFIC ANALYSES

West Springs

The West Springs AOI (Figure 15) is located in the Silver Creek drainage to the northwest of Harney Lake and near the edge of the historical phreatophytic zone. It is just downgradient from the spring-bearing basalt escarpment to the west of the Warm Springs Valley. This general area was selected, in part, due to large areas that exhibit substantial declines in NDVI. As indicated in Figure 11, the Warm Springs Valley contains one of the most extensive areas of lands with shifts in 10-year average NDVI values from above to

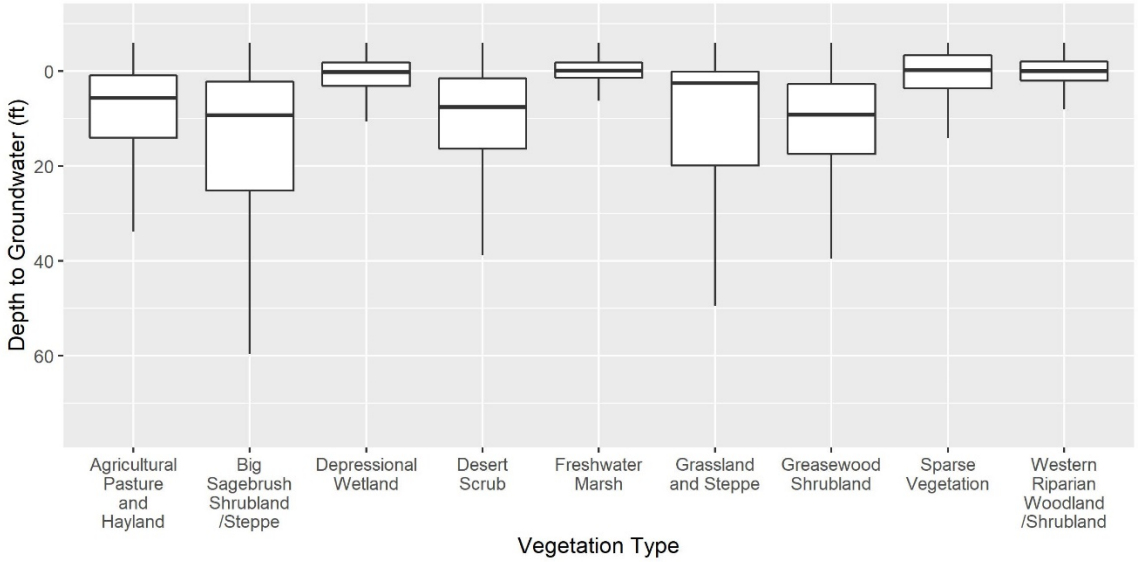

Figure 14. Ranges of estimated depths to groundwater for all pixels classified as focal vegetation types in the Harney Basin. Negative values indicate water above the land surface.

Table 2. Ranges of estimated depths to groundwater for all pixels classified as focal vegetation types in the Harney Basin phreatophyte zone. Negative values indicate water above the land surface.

Vegetation Type	Range of Groundwater Depths (ft)		
	25th Percentile	Median	75th Percentile
Agricultural Pasture and Hayland	0.9	5.6	14
Big Sagebrush Shrubland /Steppe	2.2	9.3	25.1
Depressional Wetland	-1.9	0.2	3.1
Desert Scrub	1.4	7.6	16.4
Freshwater Marsh	-1.9	-0.2	1.4
Grassland and Steppe	0.1	2.5	19.9
Greasewood Shrubland	2.7	9.1	17.4
Sparse Vegetation	-3.4	-0.2	3.6
Western Riparian Woodland /Shrubland	-2.1	0	2

below 0.3, suggesting a transition from more mesic to near-dryland conditions. Contemporary land cover classifications identify this area as a mix of *Freshwater Marsh* vegetation types intermingled with *Agricultural Pasture and Haylands*, with several areas classified as recently burned or transitional grassland types. Negative trends are evident across multiple land cover types. Positive trends are also apparent in the area, in many cases following linear pathways along canals or drainages (Figure 15).

Depths to groundwater in the closest well to the AOI (~ 3.5 km distance; HARN0052452) are 3-4 ft with only 1 year of measurement. Other wells in the vicinity have measured groundwater depths ranging from 10 to 45 ft and these show steady to slightly increasing groundwater levels (Figure 15; Well HARN0050497, Well HARN0051141, Well HARN0001304), though most have less than 5 years of data. Historical accounts identify depth to groundwater of 5 ft near the north margin of Harney Lake, and 7.5 to 10 ft at the northern end of Warm Springs Valley in Fall of 1931, with much shallower levels in the following spring, following recharge (Piper et al., 1939). Springs along the Warm Springs Valley escarpment provide an additional water source for the area but also have limited monitoring data. A recent study (Barnett, 2018) compared a compilation of historical spring discharge measurements to 2017 measurements and found that 2017 was in the lower range of the historical period of record, but did not exceed the lowest historical measurements. Consistent streamflow records for Silver Creek are not available, and thus, trends in streamflow are unknown.

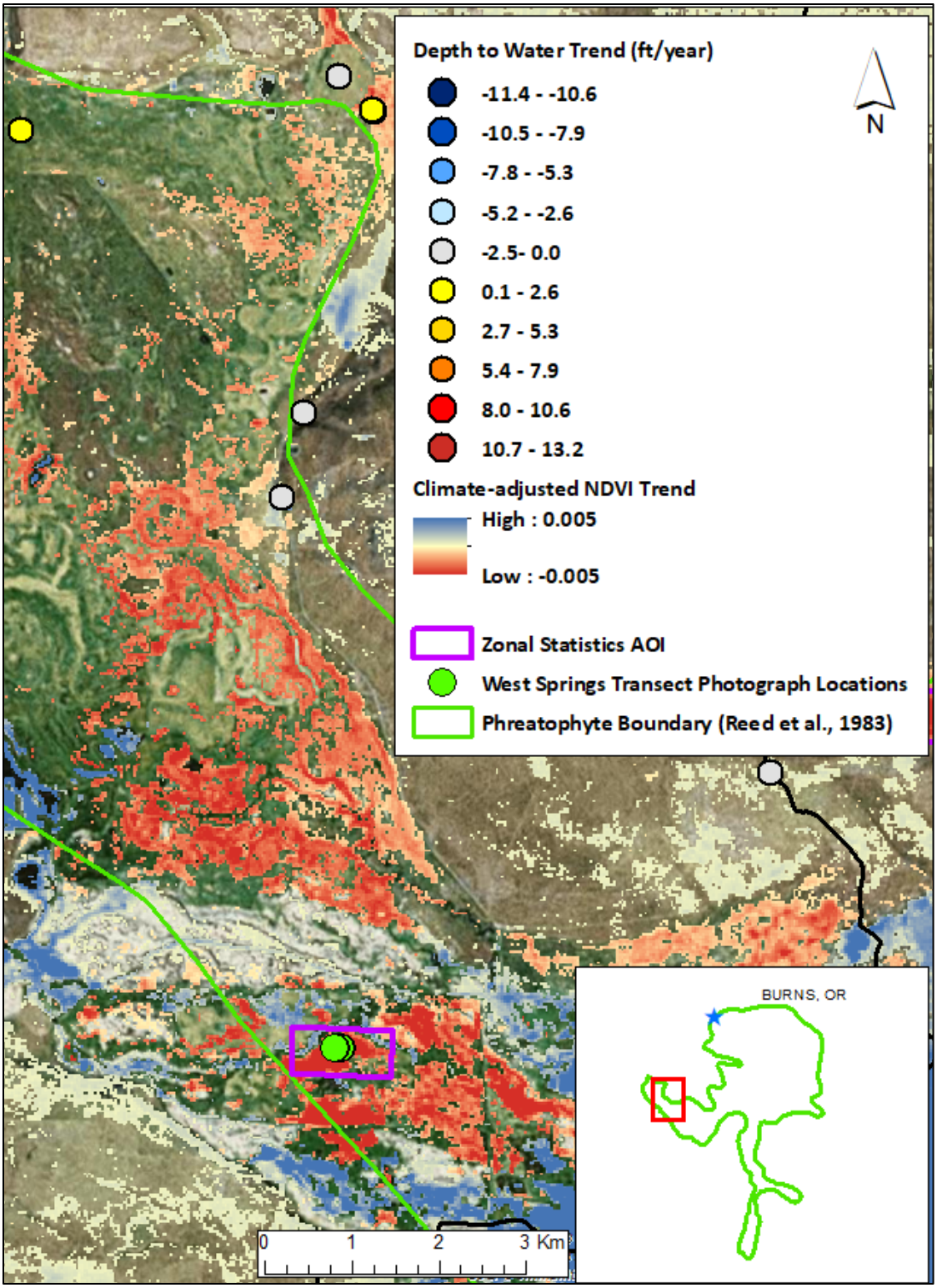

Figure 15. West Springs groundwater level and NDVI trends, site photograph locations, and AOI.

The field transect and photograph locations that were collected within this AOI (Figure 15) are located in lands classified as *Agricultural Pasture and Haylands*. Over the period of record (1985-2018), NDVI has generally been in decline (Figure 16), though relatively high NDVI values were observed in 2017. Field notes and photographs (Figure 16) from the site visit in 2019 indicate the presence of a near-monoculture of invasive plants from the Brassicaeae family, likely perennial pepperweed (*Lepidium latifolium*), given its well-documented presence as a nuisance species, including in the area near the transect (US Fish and Wildlife Service, 1995) and description as an 'intractable problem' in the study area (Christy, 2016). Graminoids were also documented to have nearly equivalent cover, with a small amount of bare ground and evidence of grazing such as trails and cow pies.

NDVI data suggest change has occurred in the West Springs AOI and the surrounding wetland complex, including large areas with declining trends in NDVI and several smaller areas with increasing trends. Due to the lack of consistent measurements of groundwater, springflows, and streamflow, it is unclear whether these changes may be a function of declining ground or surface water availability. However, the limited historical information on spring flows and groundwater depths means that current conditions might not be outside the historical range of variability. The field site visit, orthomosaic, and historical documents describing the issue of perennial pepperweed invasion together suggest that invasion by this species could plausibly be causing the observed decrease in NDVI within the transect, and possibly also in surrounding areas. Perennial pepperweed has a unique spectral signature due to its white flowers (Andrew & Ustin, 2006) and these flowerheads were still present during the site visit, although the vegetation had already mostly senesced at this time. The orthomosaic and photograph images show a distinctively less 'green' spectral signature of this species relative to surrounding vegetation. In addition, and as described in the area's habitat management plan (US Fish and Wildlife Service, 1995), several intensive management activities are ongoing, including reservoir storage, diversion, and periodic distribution of surface waters, hay and livestock production, prescribed burning, and chemical or physical control of invasive weeds. These activities are likely to strongly influence vegetation trends —both positive and negative —observed in the West Springs area. Amidst these intensive management activities, discerning the effects of changes in groundwater levels on groundwater dependent vegetation will be difficult, and doing so may require establishment of 'control' areas where effects of such changes can be monitored without being conflated by the effects of other management activities.

Weaver West

The Weaver West AOI is also located near the edge of the phreatophytic zone in the Harney Valley to the north of Harney Lake (Figure 17). Dominant vegetation classes include *Greasewood Shrubland* with interspersed *Basin Big Sagebrush Shrubland and Steppe* and *Salt Desert Scrub* vegetation types. The general area was selected due to its proximity to known groundwater declines to the northeast. The specific AOI was selected based on observations of declining vegetation trends based on the satellite imagery. The two groundwater wells in the closest vicinity of this site (1.5-3 km) have been monitored for three to five years, with HARN0051141 to the west exhibiting relatively steady levels of 35 ft over the course of 2010-2016 and HARN0051767 to the northeast showing a steady decline in depth to groundwater from 51 to 55 ft from 2016-2019. Further to the northeast, additional

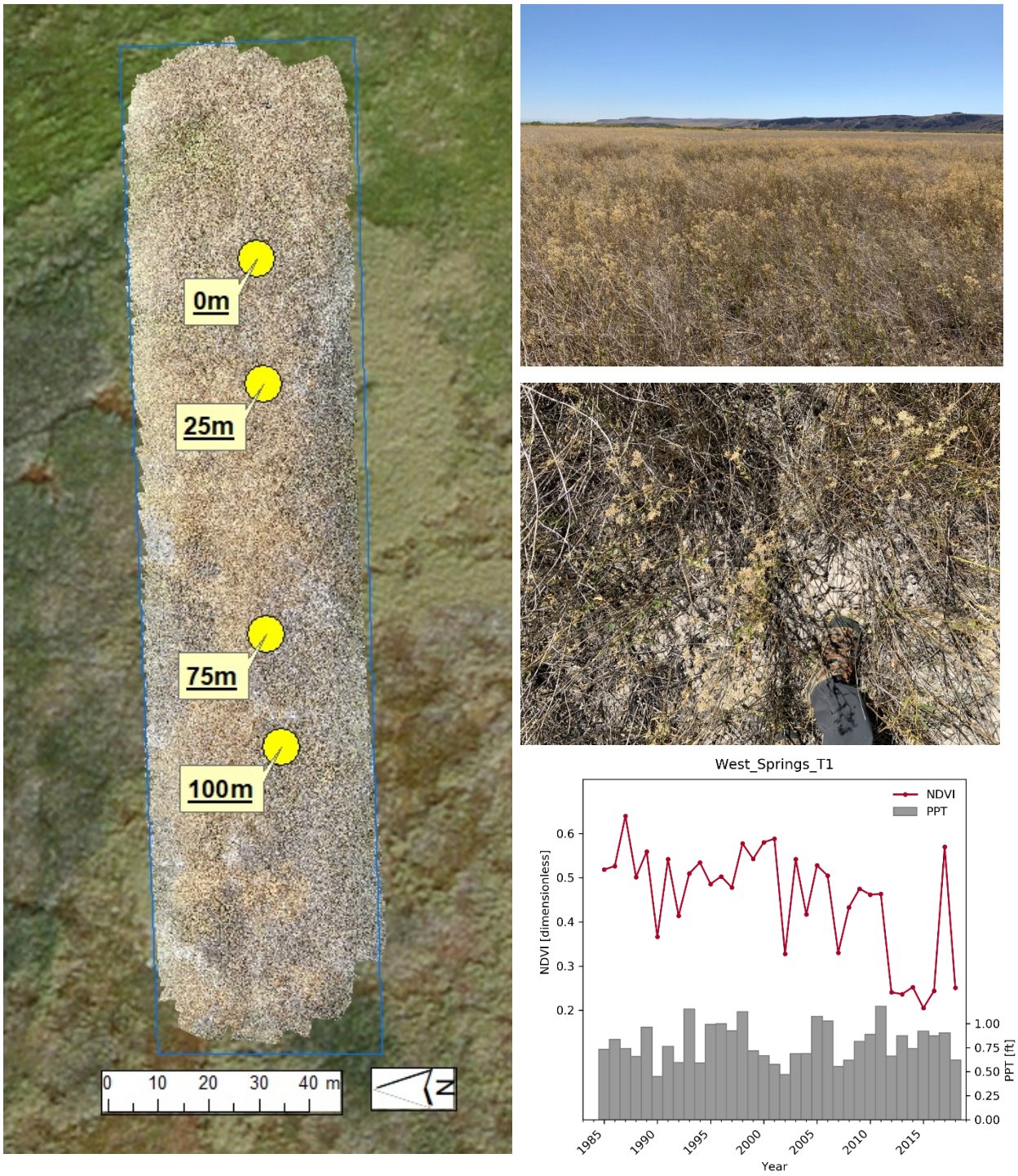

Figure 16. West Springs transect 1 UAS orthomosaic and photograph locations (left), 75m south facing ground photograph (top right), and 75m overhead ground photograph (middle right) and zonal statistics of annual NDVI and water year precipitation for the orthomosaic extent.

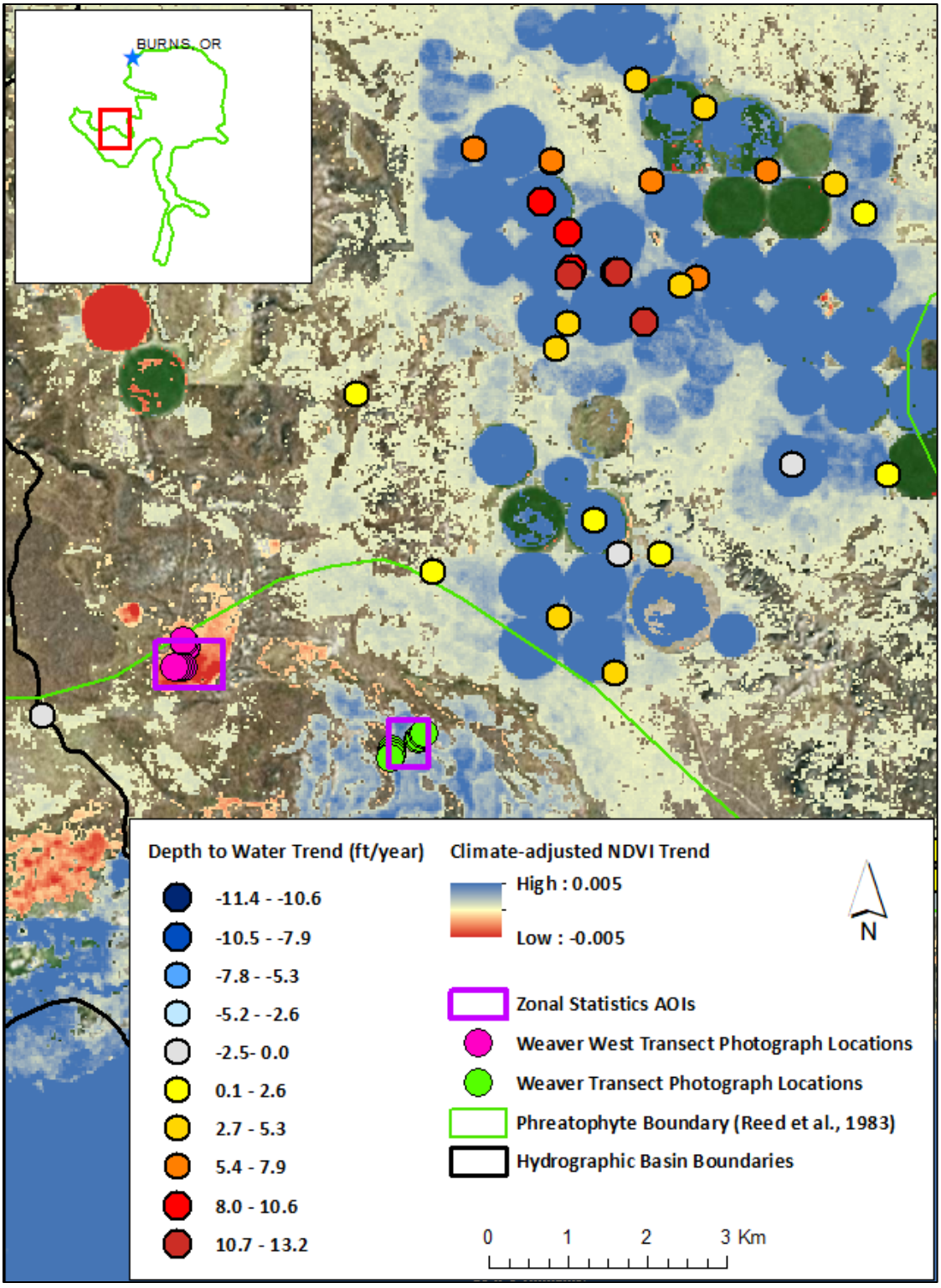

Figure 17. Weaver and Weaver West groundwater level and NDVI trends, site photograph locations, and AOIs.

wells (HARN0051146, HARN0001094, HARN00051233), document substantial increases in depth to groundwater from~ 25 to 150 ft over the course of 2006 to present. Thus, the site can be characterized as near the edge of a cone of depression (centered over most strongly declining groundwater wells and irrigated lands; Figure 17), where groundwater levels have experienced relatively recent declines.

The transect extends across lands classified as *Desert Scrubland* at the periphery of a *Greasewood Shrubland* and is in a depressional area. Field notes and photographs (Figure 18) from the site visit in 2019 indicate that the site is dominated by salt grasses (*Distichlis* sp.), non-native annual forbs, and soil crusts with only about 5 percent cover each by greasewood and bare ground. Several decaying shrub stumps and dead salt grasses were observed and existing shrubs were assigned a stress/mortality rating of two, indicating the presence of 15-49 percent dead branches. Cattle trails and cow pies were also noted. NDVI has been in steady decline over the period of record, with notably decreased interannual variability beginning in about 2001 (Figure 18). The high NDVI values at the beginning of the timeseries, along with the timeseries of Google Timelapse images (must be viewed in Google Chrome) indicate the AOI (dark area near center of image to the west of the northernmost extending arm of Harney Lake) has transitioned from mesic to dryland over the course of the study period, with the earlier mesic conditions likely remnant from the pluvial events in the mid-1980's, which caused lake and groundwater levels to rise. Observations of dead shrubs and plant stress suggest that water availability continues to decrease, and recent declines in groundwater depths warrant continued monitoring to better understand dependencies of greasewood shrubs on shallow groundwater in this area.

Weaver

The Weaver AOI is located approximately 2 km to the southeast of Weaver West in the Harney Valley and near the Harney Lake basin playa (Figure 17) The site was selected based on its land ownership and proximity to declining groundwater levels to the northeast. Landfire classifies this area as *Basin Big Sagebrush Shrubland and Steppe* with a substantial portion of *Greasewood Shrubland*. The two closest groundwater wells, within 2-3 km show steady declines in groundwater from 51-55 ft (HARN0051767) and 67 to 80 ft (HARN0001335) over the past three years, accordingly. Field notes and photographs (Figure 19) indicate that the site is dominated by invasive forbs, cheatgrass (*Bromus tectorum)*, and soil crusts, with 15 percent bare ground, 5 percent each of greasewood and grass cover and no noted presence of sagebrush (suggesting a misclassification by Landfire). A rating of one was recorded for shrub stress, indicating less than 15 percent branch mortality. The NDVI time series indicates the site was inundated by water during the first four years, had variable NDVI through the mid-1990's, followed by less-variable and slowly increasing NDVI since that time (Figure 19).

Trends at the Weaver West and Weaver sites both appear to be influenced by historically higher water levels during the early part of the time series (surface water coverage is indicated by low NDVI), followed by gradual change (Figures 18-19). As the general area was selected to understand whether declining groundwater levels may be influencing phreatophytic communities, it is worth noting that outside of the lacustrine fringe, NDVI trends in surrounding greasewood, scrub, and shrubland communities were not trending or slightly positive. Most of the natural vegetation surrounding the areas with the

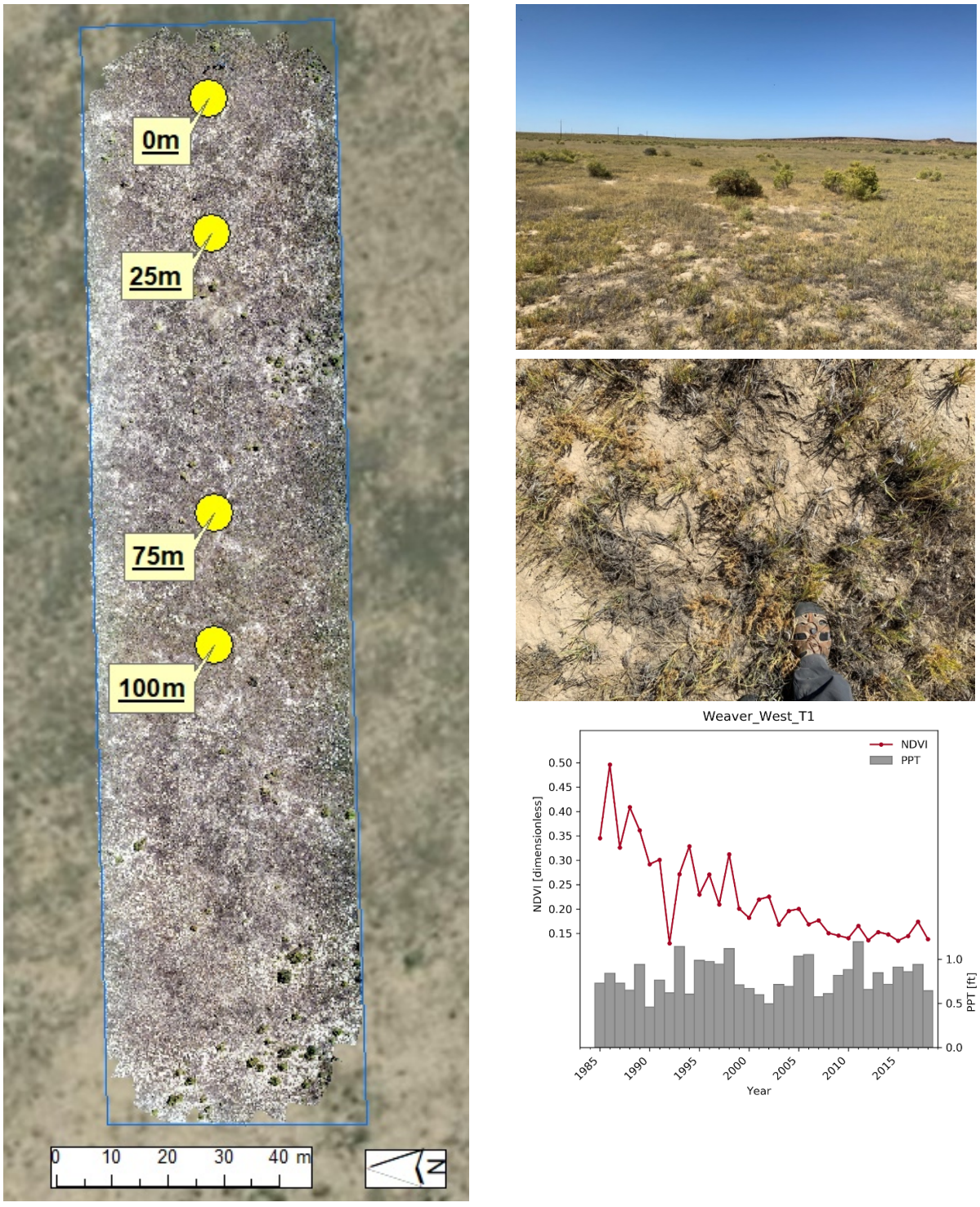

Figure 18. Weaver West transect 1 UAS orthomosaic and photograph locations (left), 25m west facing ground photograph (top right), 25m overhead ground photograph (middle right), and zonal statistics of annual NDVI and water year precipitation for the orthomosaic extent.

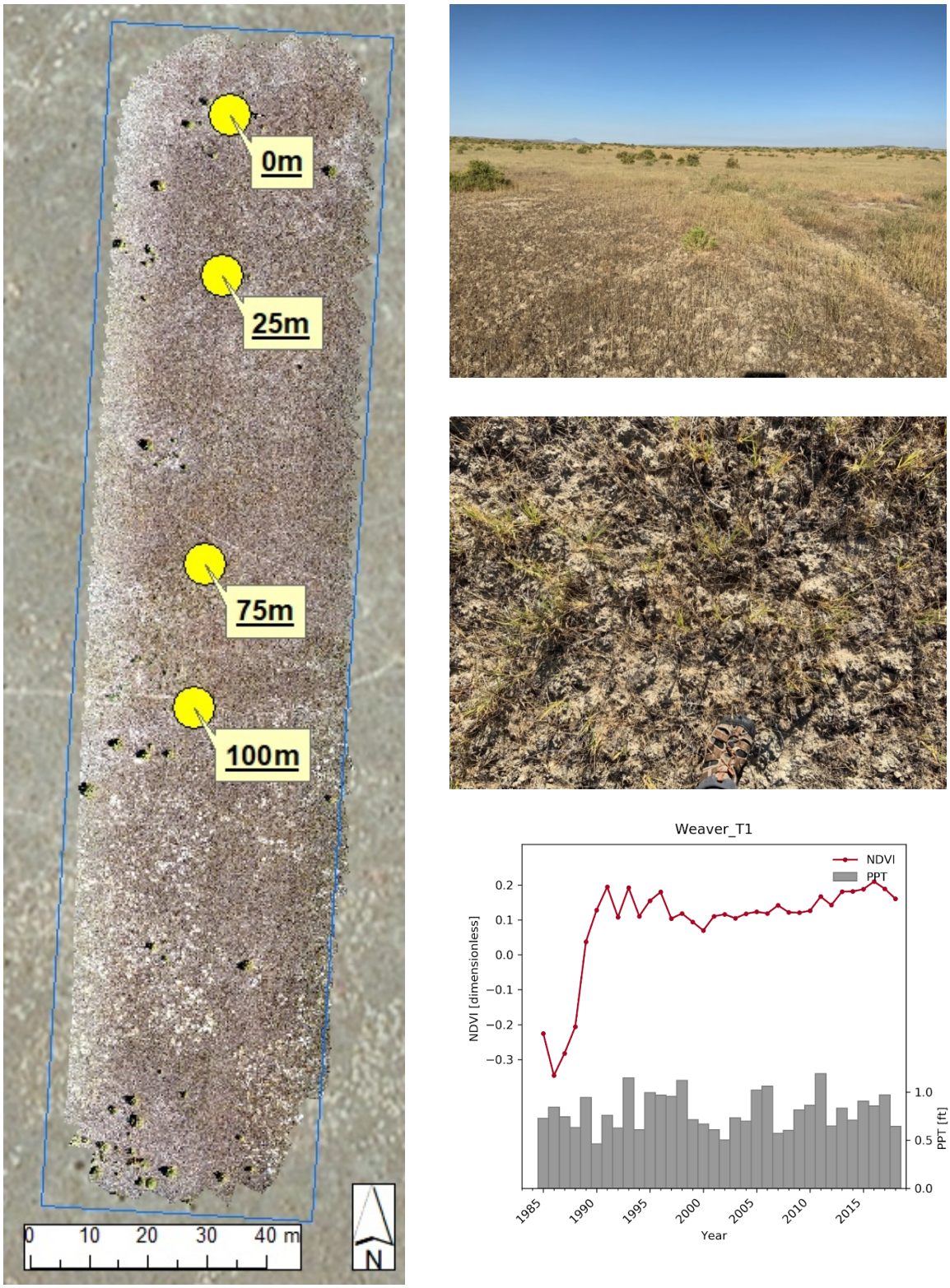

Figure 19. Weaver transect 1 UAS orthomosaic and photograph locations (left), 100m west facing ground photograph (top right), 100m overhead ground photograph (middle right), and zonal statistics of annual NDVI and water year precipitation for the orthomosaic extent.

greatest groundwater declines is classified as *Basin Big Sagebrush Shrubland and Steppe*, a community that is not typically groundwater dependent. The closest *Greasewood Shrubland* community occurs approximately 4 km from wells with the greatest increases in depth to groundwater. Well depth records along this sagebrush-greasewood ecotone (HARN00050950 HARN0051767, HARN0051141) are in the range of 35-50 ft and declining at rates of about 1 ft per year over the past three years in the cases of the former two. It is plausible that if greasewood in this community are groundwater dependent, the effects of declining groundwater levels have not yet occurred, as groundwater depths remain within the range of those documented for this species (Nichols, 1994). The persistence of greasewood will depend on whether precipitation is sufficient to sustain the water needs of this species and, if not, whether root growth rates can keep pace with groundwater declines (Naumburg et al., 2005).

Malheur North

The Malheur North AOI is located at the southern edge of Malheur Lake, near the MNWR visitor center (Figure 20) and was selected on the basis of declining trends observed along the lacustrine fringe. The area includes *Basin Big Sagebrush Shrubland and Steppe*, *Riparian Woodland and Shrubland*, *Agricultural Pasture and Haylands*, and *Sparse Vegetation* types. Groundwater levels at the nearest well (1.5 km away, HARN0001363) have been monitored on a relatively continuous basis since 1965 and range from 2-9 ft, but show declines in water table elevation below the historic range of variability since 2011.

Like the Weaver West AOI, the area was likely influenced by pluvial conditions in the mid-1980's and NDVI timeseries (Figure 21) and Google Timelapse timeseries (must be viewed in Google Chrome) indicate mesic conditions (NDVI > 0.5) that have transitioned toward drier conditions over the course of the study period. Field observations along the transect indicate the site is now dominated by dense stands of greasewood, rabbitbrush, and seeded grass species (and possibly misclassified by Landfire). Both greasewood and rabbitbrush showed signs of drought stress (rating = 2), as indicated by 15-49 percent dead branches.

Malheur South

The Malheur South AOI straddles the widespread declining vegetation trends adjacent to the Donner und Blitzen River, approximately 4 km southeast of the Malheur North AOI (Figure 20). Dominant land cover types include *Agricultural Pasture and Haylands*, *Riparian Woodland and Shrubland*, and *Basin Big Sagebrush Shrubland and Steppe*. Nearby groundwater wells 3 km to the northwest (HARN0001467) and 3.5 km to the southeast (HARN0051387) show declining trends with depths ranging from 13-15 ft and 23-28 ft in the past 5 to 10 years, respectively. Stream baseflows in the Donner und Blitzen show no apparent trend over the 2006-2013 period of record (Kormos et al., 2016).

This AOI was selected based on its accessibility and being representative of declining NDVI trends that are apparent along several miles of the Donner und Blitzen floodplain. The transect site is along the edge of a dry channel paralleling the river, that is classified by Landfire as open water. Aerial imagery from 2016 confirms the presence of water in the channel at the time it was collected but water was not present during Fall 2019 (Figure 22).

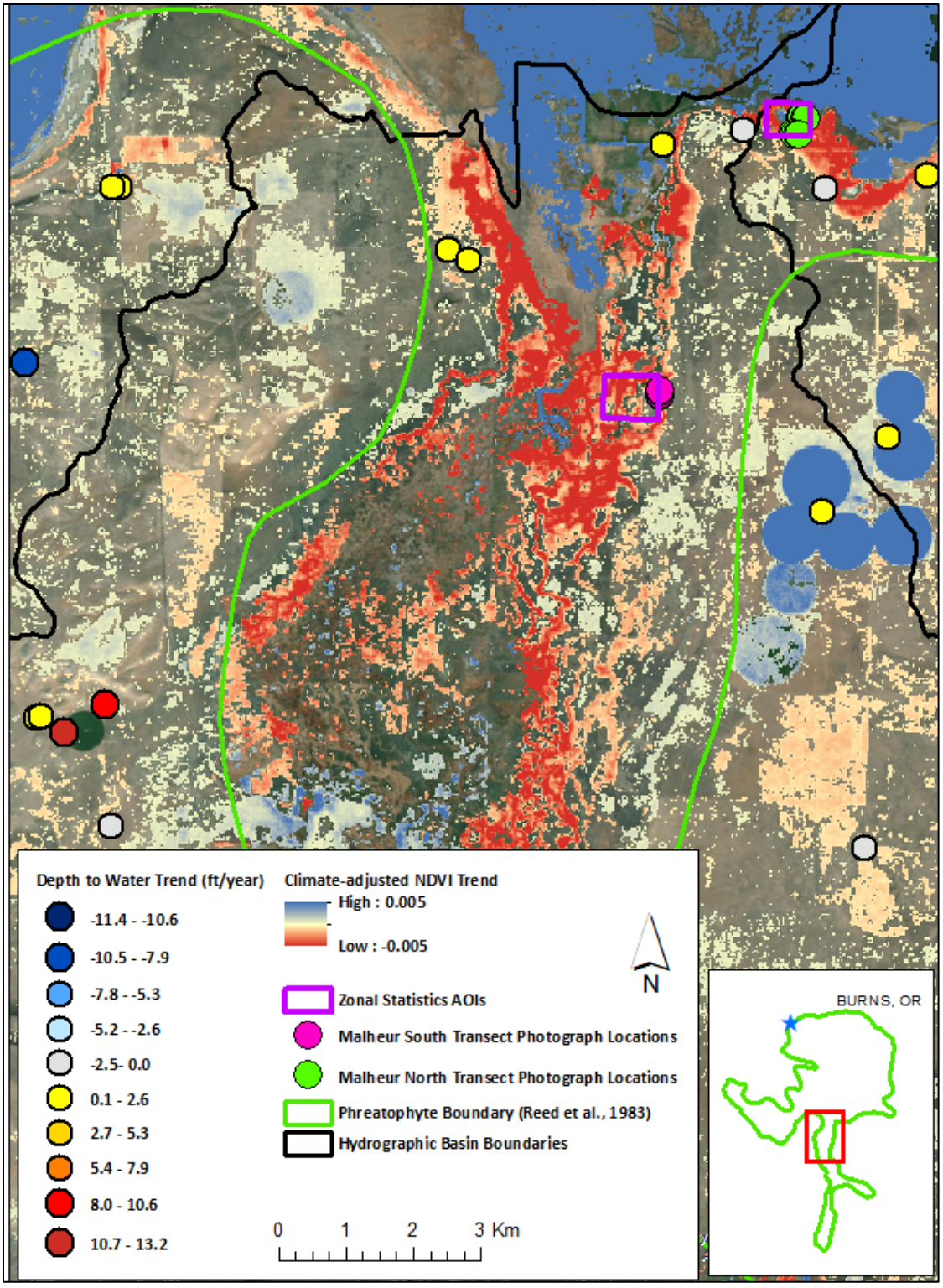

Figure 20. Malheur North and Malheur South groundwater and NDVI trends, site photograph locations, and AOI's.

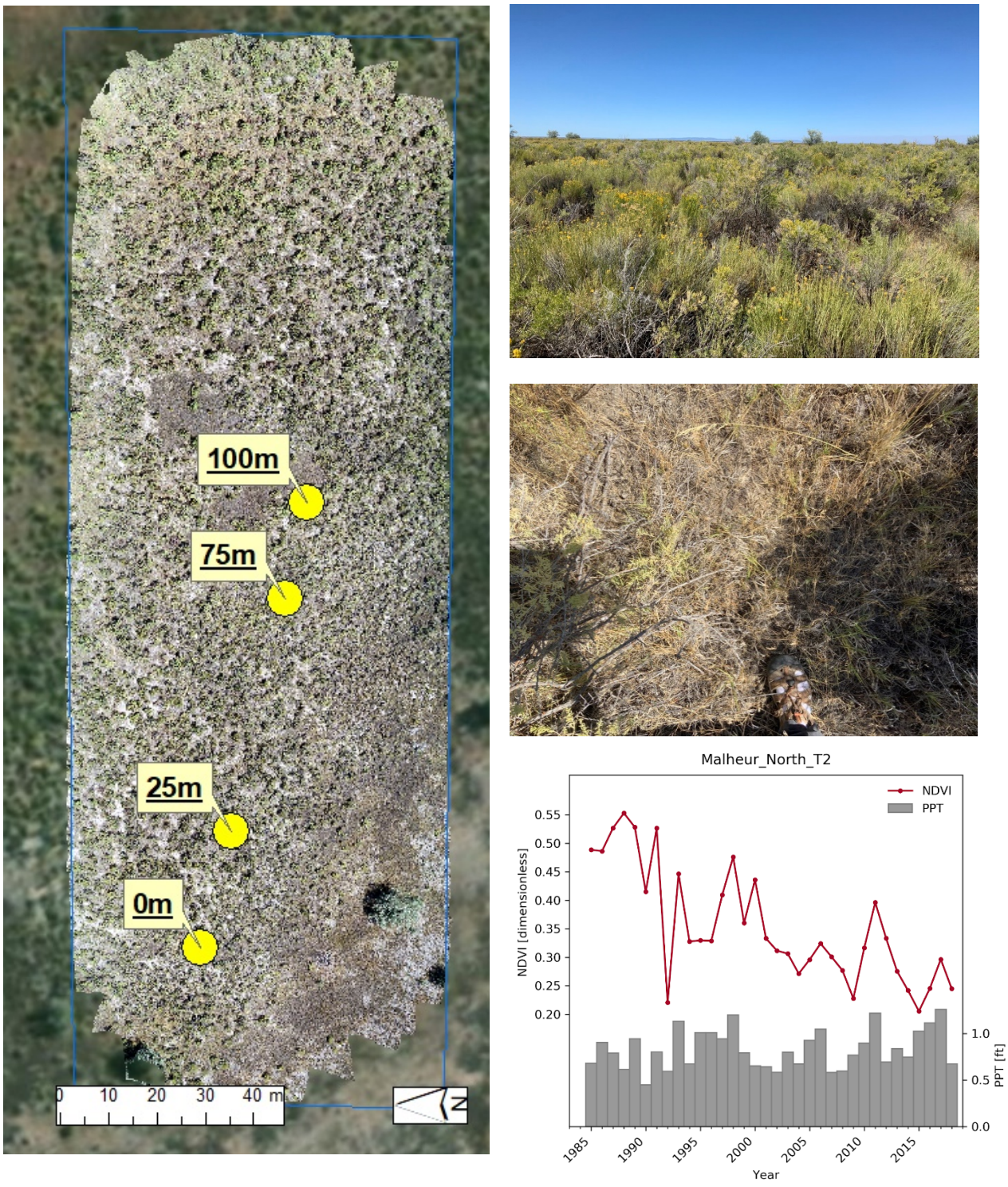

Figure 21. Malheur North transect 2 UAS orthomosaic and photograph locations (left), 25m north facing ground photograph (top right), 25m overhead ground photograph (middle right), and zonal statistics of annual NDVI and water year precipitation for the orthomosaic extent.

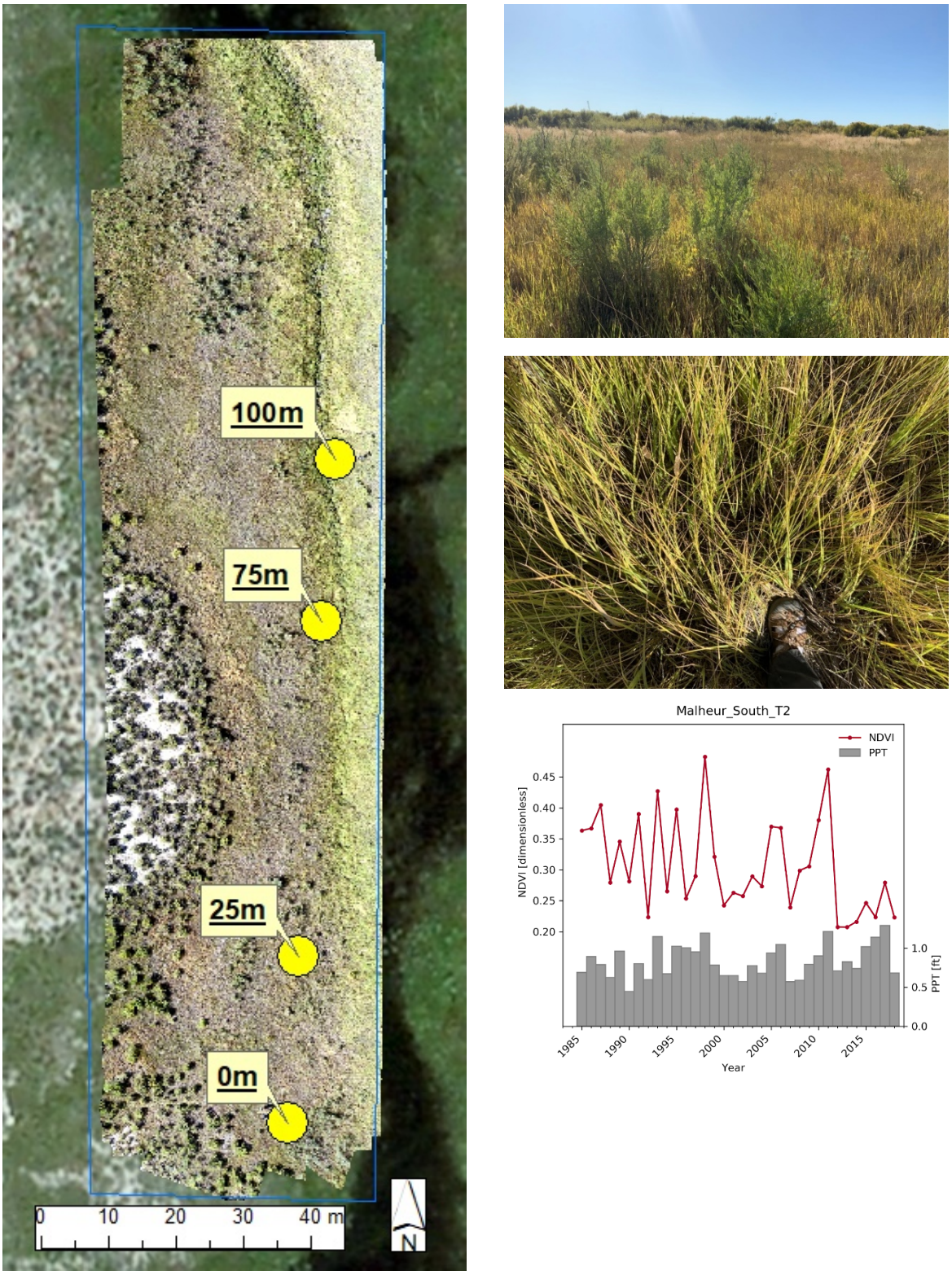

Figure 22. Malheur South transect 2 UAS orthomosaic and photograph locations (left), 75m west facing ground photograph (top right), 75m overhead ground photograph (middle right), and zonal statistics of annual NDVI and water year precipitation for the orthomosaic extent.

The Google Timelapse timeseries (must be viewed in Google Chrome; AOI is to the east of the main river channel, due west of the northernmost agricultural plot that appears in the time series in 2003) shows substantial interannual variability in the spectral characteristics of the AOI that are driven by changes in water extent (dark areas indicate water). The site was densely vegetated with graminoids, mostly *Carex spp*. (65% cover), with willow and rabbitbrush interspersed along the edges of the channel. Willow species showed signs of drought stress (rating = 2, as indicated by 15-49 percent branch mortality), while rabbitbrush appeared healthy. It is possible the observed willow stress could be due to grazing pressure. Signs of livestock grazing such as cow pies and trailing were also evident. NDVI trends along the transect and in the AOI generally indicate declines over the course of the study period, amid substantial interannual variability that tracked closely with precipitation. Spatial patterning of negative trends track closely with land cover classifications of open water channels and *Agricultural Pasture and Haylands* in some places, but also extend across areas classified as *Basin Big Sagebrush Shrubland and Steppe*. As with the West Springs area, the Donner und Blitzen is an area that is heavily managed with extensive surface water manipulations, selective flooding, hay and livestock production, prescribed fire, and mowing activities that are likely influencing vegetation in this area in a variety of ways that have the potential to obscure the influences of declining groundwater levels.

Frenchglen North

The Frenchglen North AOI is located along the western edge of the phreatophyte zone along a channelized section of the Donner and Blitzen River, near Frenchglen (Figure 23). The transect was located outside the AOI, as the AOI was determined to be inaccessible upon visiting the sites. The transect was instead located 0.3 km north of Well HARN 0050612, approximately 1 km north of the northern end of the AOI, in a transition zone between lands classified as wetland and sagebrush shrubland vegetation types. Water levels in the area have only been measured in recent years, and range between 1-2 ft, with slightly deeper water levels of 3-4 ft to the north of the transect, in Well HARN0050598 and no apparent trends. The areas to the east of the transect are classified almost entirely as *Freshwater Marsh*, with an extensive network of canals, signs of hay harvesting, and prescribed fire likely influencing the trends in this area. Vegetation along the transect was dominated by greasewood (~30% cover; another Landfire misclassification) but transitioned into wetland vegetation toward the northern end. Greasewood showed no signs of water stress and other cover types included seeded species, bare ground, and soil crusts. Signs of fire and mowing were observed within the transect, though NDVI was only subtly declining (Figure 24).

Frenchglen South

The Frenchglen South transects were located along the southernmost end of the phreatophyte boundary and the Warm Springs canal, outside the originally designated AOI (Figure 23), which did not contain groundwater dependent vegetation. The nearest groundwater well is approximately 7.5 km to the north, adjacent to the Frenchglen North AOI. The area surrounding the transects is mostly classified as *Big Sagebrush Shrubland and Steppe* with areas classified as invasive annual grassland, including along both transects. Field photographs (Figure 25) and data confirmed the presence of invasive Brassicaceae

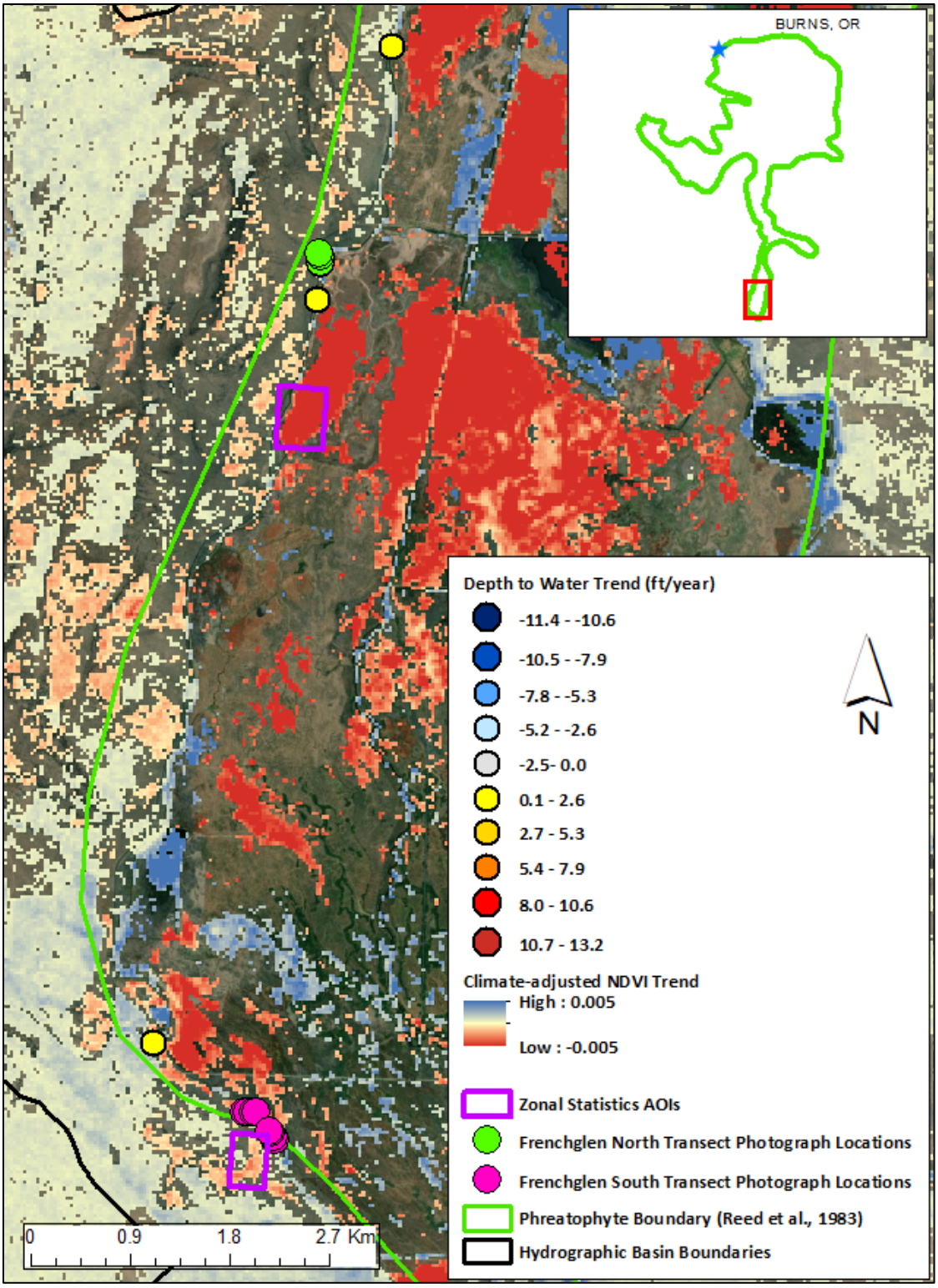

Figure 23. Frenchglen North and Frenchglen South groundwater and NDVI trends, site photograph locations, and AOI's.

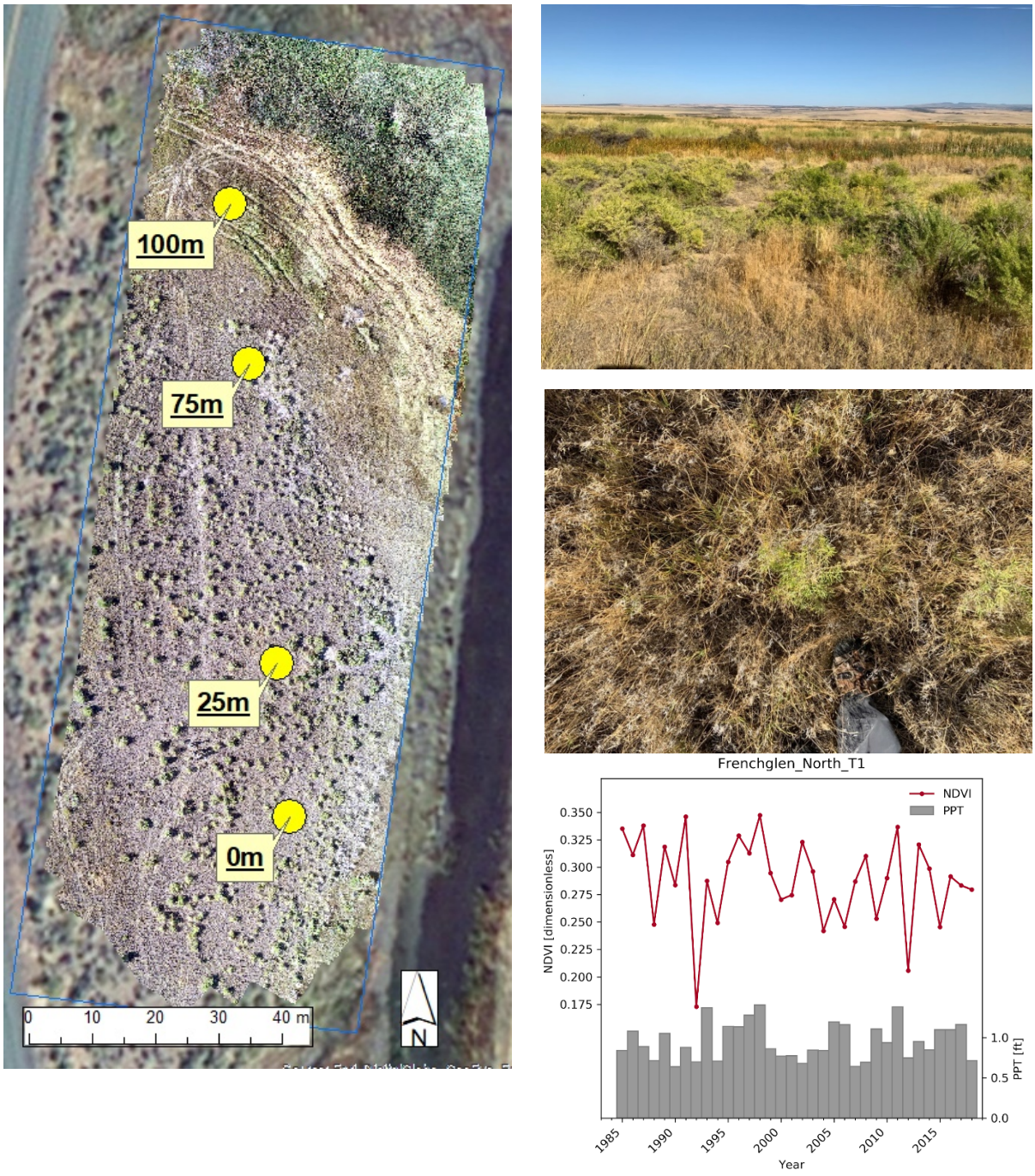

Figure 24. Frenchglen North transect 1 UAS orthomosaic and photograph locations (left), 25m east facing ground photograph (top right), 25m overhead ground photograph (middle right), and zonal statistics of annual NDVI and water year precipitation for the orthomosaic extent.

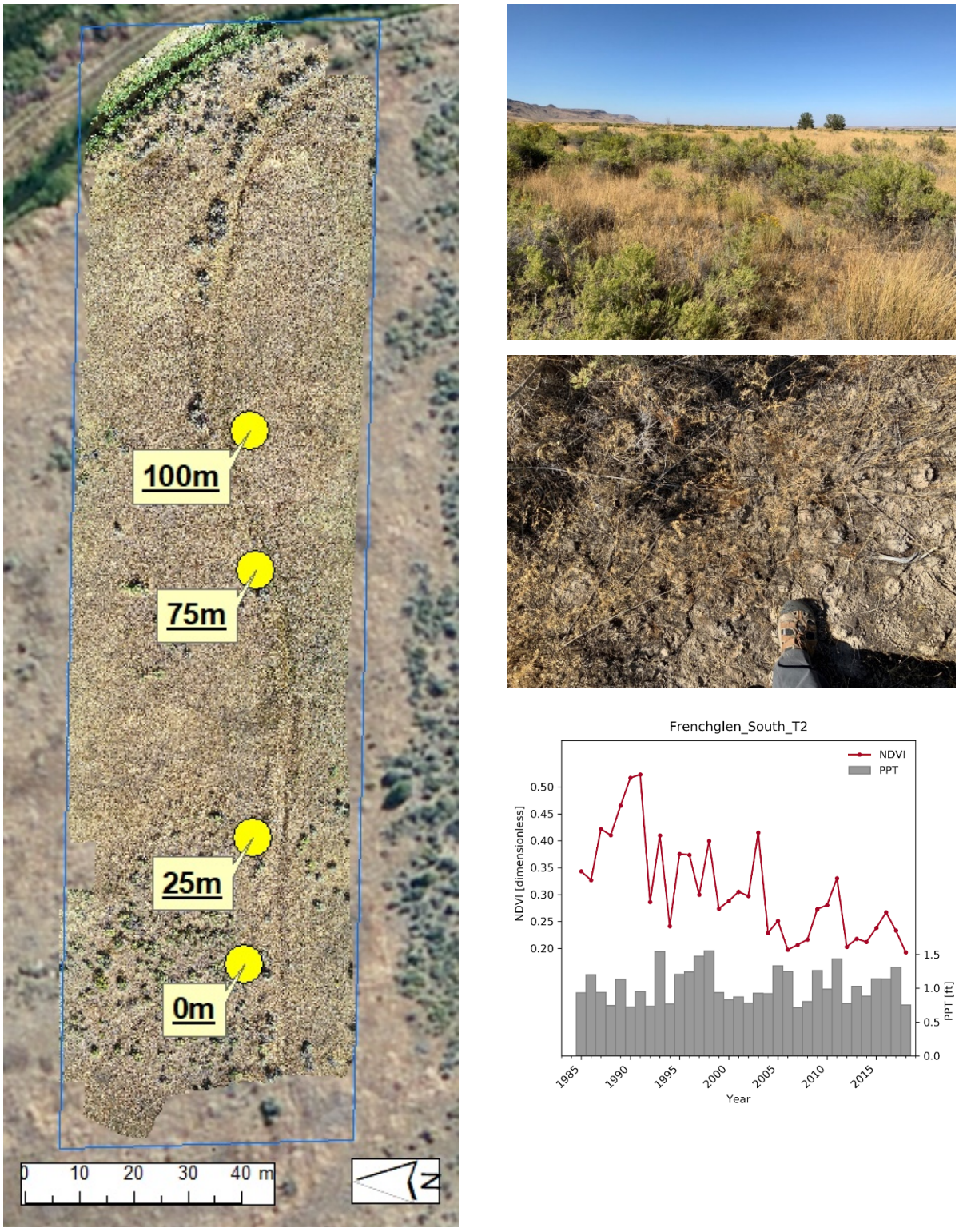

Figure 25. Frenchglen South transect 2 UAS orthomosaic and photograph locations (left), 0m north facing ground photograph (top right), 0m overhead ground photograph (middle right), and zonal statistics of annual NDVI and water year precipitation for the orthomosaic extent.

(likely small whitetop (*Lepidium draba*) or perennial pepperweed), cheatgrass, and large stands of invasive thistle (collectively comprising 30% of cover), in addition to shrubs such as rabbitbrush, greasewood, and sagebrush (collectively comprising 15% of cover). These shrub species showed signs of moderate water stress (rating = 2; 15- 49 percent branch mortality). Observed declines in NDVI (Figure 25) may be associated with water stress or non-native species invasion.

The limited groundwater data for the Frenchglen North area indicate shallow groundwater depths capable of supporting extensive wetland vegetation, though groundwater data for the Frenchglen South area are not available and wells associated with Frenchglen North are too far away to be reliable. Cropland irrigation that might affect groundwater in this area is absent in adjacent areas, suggesting groundwater levels in this area are unlikely to be drawn down by groundwater pumping. As with other areas within the refuge, evidence of significant vegetation management such as flooding, mowing, burning, river channelization and other types of water diversions are likely to strongly influence the NDVI trends observed in the area. These have the potential to obscure the impacts of changing ground or surface water levels on vegetation. Indeed, areas of increasing and decreasing NDVI trends tended to follow road and canal boundaries, suggesting the influence of controlled management activities.

CONCLUSIONS

In this report, we examine historical and current relations between groundwater dependent vegetation, shallow groundwater and climate using a combination of gridded satellite remote sensing and climate data (1985-2018) and field observations of vegetation and groundwater levels. Here we highlight key findings from the analysis:

1) Widespread declines in shallow groundwater levels are evident (Figure 4). In wells with at least 3 years of observations, trend analyses indicate declining groundwater levels, with most wells exhibiting declines on the order of 0-2.5 ft/yr, but some declining at a rate of greater than 5 ft/yr. 'Hotspots' of groundwater declines include the Weaver Springs area to the northwest of Malheur Lake, and in the northeasternmost corner of the alluvial valley. Groundwater declines are less evident in the Frenchglen and West Springs areas, where shallow groundwater levels persist.
2) Declines in groundwater levels in most wells are independent of antecedent (6-36 month) climate conditions (Figures 5-6). Antecedent climate was strongly correlated with groundwater levels in only about 30 percent of the subset of wells selected for partial correlation analysis. These wells tended to have shallower depths to groundwater and were located along the mountain front where recharge occurs. In contrast, 80 percent of the subset of wells included in the partial correlation analysis, which controlled for antecedent climate effects, showed downward trends over time that are independent of short-term climate. Trends in wells with depths to groundwater > 60 ft were especially strong.

3) Large areas of the study area showing positive trends in NDVI actually reflected receding water levels and conversion to irrigated cropland rather than increases in vegetation vigor of native/riparian communities (Figures 7-10).

4) Negative trends in vegetation vigor were most prominent in localized patches within mesic (*Freshwater Marsh, Depressional Wetland, Riparian Woodland and Shrubland),* and *Agricultural Pasture and Hayland* vegetation types (Figure 8). However, in aggregate, ranges of NDVI values for each vegetation type did not differ substantially between the start and end of the study period (Figure 9).

5) Wetland and riparian vegetation types exhibit distinctive interquartile ranges of NDVI values that can be useful for monitoring transitions from mesic to dryland or otherwise disturbed conditions (Figure 10). Using a threshold of NDVI>=0.3 as a determinant of mesic conditions, transition 'hotspots' of mesic vegetation over the course of the study period are identified in the Warm Springs Valley, along the southern periphery of Malheur Lake and terminus of the Donner und Blitzen River, and in the vicinity of Poison Creek and Ninemile Sloughs in the northern part of the study area (Figure 11).

6) Preliminary estimates of groundwater depths associated with different vegetation types may provide the basis for initial benchmarks of groundwater depths needed to maintain groundwater dependent vegetation (Figure 14). This information can be updated once a more comprehensive analysis of water table depths is available.

7) Site-specific analyses of field and remote sensing data identified transitions from mesic to dryland vegetation in the lacustrine fringe that appears to be in response to declining lake levels since the 1980's of Malheur and Harney Lakes (Weaver West, Weaver, Malheur North). That said, the recent declines in groundwater levels observed in these areas could also be playing a role as lake levels and groundwater levels are inextricably linked to each other. Other field sites where trends in vegetation were evident (West Springs, Frenchglen) have limited evidence of groundwater declines and are places where monocultures of invasive species were observed and intensive vegetation management activities such as mowing, prescribed fire, invasive plant management, and manipulation of water levels are likely influencing vegetation trends. In places where both groundwater and vegetation declines are occurring (Malheur North and South), such management activities may be obscuring the connections between trends in groundwater depth and trends in vegetation. Establishing control areas where natural changes in vegetation in association with depth to groundwater can be monitored would help to alleviate these confounding factors of lake level changes and land management activities

8) These results emphasize the importance of water- and land management as determinants of the abundance and distribution of groundwater-dependent vegetation. Holistic, beneficial management actions that are targeted to support groundwater-dependent vegetation may be able to offset the water stress due to regional groundwater withdrawal.

In this study, we demonstrate a set of approaches for understanding relations between climate, depth to groundwater, and vegetation vigor of groundwater dependent vegetation communities. Understanding vegetation responses in the contexts of variable climate and groundwater is essential for quantifying current status and for monitoring past or future trends in response to changing management. The approaches described here could be readily applied to other study areas where planning objectives include consideration of sustainability of groundwater dependent ecosystems. As ongoing groundwater studies of the Harney Basin generate new information on historical or predicted future changes in shallow groundwater depth, results from our study could be further analyzed to understand past and potential future responses of groundwater dependent vegetation to these changes. For example, timeseries of model-generated potentiometric surfaces could be used to correlate with remotely sensed vegetation indices to more precisely understand how they covary over space and time within the study area and to understand implications of reduced water levels to vegetation. Such analyses may be particularly useful for understanding how ground and surface water interactions may be driving observed changes in groundwater dependent vegetation in the lacustrine fringe.

REFERENCES

Abatzoglou, J. T. (2013). Development of gridded surface meteorological data for ecological applications and modelling. *International Journal of Climatology*, *33*(1), 121–131. https://doi.org/10.1002/joc.3413

Albright, W. H., Jasoni, R. L., Cablk, M. E., Thomas, J. M., Decker, D. L., & Arnone, J. A. (2006). Evapotranspiration in Smoke Creek Desert, Nevada. Desert Research Institute Publication Number 41224.

Allen, R., Walter, I., Elliott, R., Howell, T., Itenfisu, D., Jensen, M., & Snyder, R. (2005). The ASCE standardized reference evapotranspiration equation. Reston, VA:American Society of Civil Engineers.

Alley, W. M. (1988). Using exogenous variables in testing for monotonic trends in hydrologic time series. *Water Resources Research*, *24*(11), 1955–1961. https://doi.org/10.1029/WR024i011p01955

Andrew, M., & Ustin, S. (2006). Spectral and physiological uniqueness of perennial pepperweed (Lepidium latifolium). *Weed Science - WEED SCI*, *54*, 1051–1062. https://doi.org/10.1614/WS-06-063R1.1

Barnett, H. (2018). Determining the Spring Water Provenance in the Warm Springs Valley Subarea of the Silver Creek Watershed in the Harney Hydrologic Basin, Harney County, Oregon. MESSAGe Technical Report Number: 060. https://doi.org/10.1017/CBO9781107415324.004

Beamer, J. P., Huntington, J. L., Morton, C. G., & Pohll, G. M. (2013). Estimating Annual Groundwater Evapotranspiration from Phreatophytes in the Great Basin Using Landsat and Flux Tower Measurements. *Journal of the American Water Resources Association*, *49*(3), 518–533. https://doi.org/10.1111/jawr.12058

Bredefoeft, J. (2002). The Water Budget Myth Revisited: Why Hydrogeologists Model. *Groundwater*, *40*(4).

Childress, W., Price, D., Codren, C., & McLendon, T. (1999). A functional description of the Ecological Dynamics Simulation (EDYS) Model, with applications for army and other federal land managers. USACE CERL Technical Reports 99/55.

Chimner, R., & Cooper, D. (2004). Using stable oxygen isotopes to quantify the water source used for transpiration by native shrubs in the San Luis Valley, Colorado U.S.A. *Plant and Soil*, *260*, 225–236.

Christy, J. A. (2016). Wet Meadow Plant Associations, Double O Unit, Malheur National Wildlife Refuge, Harney County, Oregon. Institute for Natural Resources Publications. 34. Retrieved from https://pdxscholar.library.pdx.edu/naturalresources_pub/34

Cooper, D. J., Sanderson, J. S., Stannard, D. I., & Groeneveld, D. P. (2006). Effects of long-term water table drawdown on evapotranspiration and vegetation in an arid region phreatophyte community. *JOURNAL OF HYDROLOGY*, *325*(3995), 21–22. https://doi.org/10.1016/j.jhydrol.2005.09.035

Dawson, T. E., & Pate, J. S. (1996). Seasonal water uptake and movement in root systems of Australian phraeatophytic plants of dimorphic root morphology: a stable isotope investigation. *Oecologia*, *107*, 13–20.

Donnelly, J. P., Naugle, D. E., Hagen, C. A., & Maestas, J. D. (2016). Public lands and private waters: Scarce mesic resources structure land tenure and sage-grouse distributions. *Ecosphere*, *7*(1), 1–15. https://doi.org/10.1002/ecs2.1208

Elmore, A. J., Mustard, J. F., & Manning, S. J. (2003). Regional patterns of plant community response to changes in water: Owens Valley, California. *Ecological Applications*, *13*(2), 443–460. https://doi.org/10.1890/1051-0761(2003)013[0443:RPOPCR]2.0.CO;2

Garcia, C. A., Huntington, J. M., Buto, S. G., Moreo, M. T., Smith, J. L., & Andraski, B. J. (2015). *Groundwater Discharge by Evapotranspiration , Dixie Valley , West-Central Nevada , March 2009 – September 2011*. *Professional Paper 1805*.

Gorelick, N., Hancher, M., Dixon, M., Ilyushchenko, S., Thau, D., & Moore, R. (2017). Google Earth Engine: Planetary-scale geospatial analysis for everyone. *Remote Sensing of Environment*, *202*, 18–27. https://doi.org/https://doi.org/10.1016/j.rse.2017.06.031

Groeneveld, D. P., Baugh, W. M., Sanderson, J. S., & Cooper, D. J. (2007). Annual groundwater evapotranspiration mapped from single satellite scenes. *Journal of Hydrology*, *344*(1–2), 146–156. https://doi.org/10.1016/j.jhydrol.2007.07.002

Hamed, K., & Rao, R. (1998). A modified Mann-Kendall trend test for autocorrelated data. *Journal of Hydrology*, *204*, 182–196. https://doi.org/10.1200/jco.2018.36.15_suppl.522

Helsel, D. R., & Hirsch, R. M. (2002). Chapter 12 Trend Analysis. *Statistical Methods in Water Resources*, 323–355.

Hobbins, M., & Huntington, J. L. (2016). Evapotranspiration and Evaporative Demand. In V. Singh (Ed.), *Handbook of Applied Hydrology* (2nd ed., pp. 42.1-42.18). New York, NY: McGraw-Hill Publishing. https://doi.org/10.1061/9780784415177.ch03

Huntington, J., McGwire, K., Morton, C., Snyder, K., Peterson, S., Erickson, T., et al. (2016). Assessing the role of climate and resource management on groundwater dependent ecosystem changes in arid environments with the Landsat archive. *Remote Sensing of Environment*, *185*, 186–197. https://doi.org/10.1016/j.rse.2016.07.004

Kendall, M. G. (1975). *Rank Correlation Methods*. Griffin, London, UK.

Kim, S. (2015). Partial and Semi-Partial (Part) Correlation: Package ‘ ppcor ,’ 1–9.

Kormos, P., Luce, C., Wenger, S., & Berghuijs, W. (2016). Trends and sensitivities of low streamflow extremes to discharge timing and magnitude in Pacific Northwest mountain streams. *Water Resources Research*, *52*, 4990–5007. https://doi.org/10.1111/j.1752-1688.1969.tb04897.x

Mann, H. B. (1945). Nonparametric Tests Against Trend. *Econometrica*, *13*(3), 245–259. https://doi.org/10.2307/1907187

McGwire, K., Minor, T., & Fenstermaker, L. (2000). Hyperspectral mixture modeling for quantifying sparse vegetation cover in arid environments. *Remote Sensing of Environment*, *72*(3), 360–374. https://doi.org/10.1016/S0034-4257(99)00112-1

Naumburg, E., Mata-Gonzalez, R., Hunter, R. G., McLendon, T., & Martin, D. W. (2005). Phreatophytic vegetation and groundwater fluctuations: A review of current research and application of ecosystem response modeling with an emphasis on great basin vegetation. *Environmental Management*, *35*(6), 726–740. https://doi.org/10.1007/s00267-004-0194-7

Nichols, W. D. (1994). Groundwater discharge by phreatophyte shrubs in the Great Basin as related to depth to groundwater. *Water Resources Research*, *30*(12), 3265–3274. https://doi.org/10.1029/94WR02274

Patakamuri, S., & O'Brien, N. (2020). modifiedmk: Modified Versions of Mann Kendall and Spearman's Rho Trend Tests version 1.5.0.

Patten, D. T., Rouse, L., & Stromberg, J. C. (2008). Isolated spring wetlands in the Great Basin and Mojave deserts, USA: Potential response of vegetation to groundwater withdrawal. *Environmental Management*, *41*(3), 398–413. https://doi.org/10.1007/s00267-007-9035-9

Peña, E. A., & Slate, E. H. (2006). Global Validation of Linear Model Assumptions. *Journal of the American Statistical Association*, *101*(473), 341. https://doi.org/10.1198/016214505000000637

Piper, A., Robinson, T. W., Park, C. F., & Jessup, L. T. (1939). Geology and ground-water resources of the Harney Basin, Oregon, with a statement on Precipitation and tree growth. Water Supply Paper 841.

Reed, J., Bedinger, M., Gonthier, J., & McFarland, W. (1984). Maps showing groundwater units and number of large-capacity wells, Basin and Range Province, Oregon. Water Resources Investigations Report 83-4120-A.

Robinson, T. (1958). Phreatophytes. *Geological Survey Water Supply Paper 1423*. https://doi.org/10.1007/978-3-642-41714-6_161334

Schmidt, G., Jenkerson, C., Masek, J., Vermote, E., & Gao, F. (2013). Landsat Ecosystem Disturbance Adaptive Processing System (LEDAPS) Algorithm Description. *USGS Open-File Report 2013–1057*.

Sen, P. K. (1968). Estimates of the Regression Coefficient Based on Kendall's Tau. *Journal of the American Statistical Association*, *63*(324), 1379–1389. https://doi.org/10.1080/01621459.1968.10480934

Smith, R., & Roe, W. (2019). Oregon Geologic Data Compilation, release 6. Retrieved from https://www.oregongeology.org/pubs/dds/p-OGDC-6.htm

Stromberg, J., Tiller, R., & Richter, B. (1996). Effects of Groundwater Decline on Riparian Vegetation of Semiarid Regions : The San Pedro. *Ecological Applications*, *6*(1), 113–131.

U.S. Department of Interior, U. S. G. S. (2016). LANDFIRE Existing Vegetation Type; LF Remap/LF 2.0.0. Retrieved December 20, 2019, from https://www.landfire.gov/viewer/

U.S. Geological Survey. (2019). Landsat 8 Surface Reflectance Code (LASRC) Poduct Guide. (No. LSDS-1368 Version 2.0)., (May), 40. Retrieved from https://www.usgs.gov/media/files/landsat-8-surface-reflectance-code-lasrc-product-guide

U.S. Geological Survey (USGS). (2018). Landsat Dynamic Surface Water Extent (DSWE) Product Guide Version 2.0. Sioux Falls, South Dakota.

US Fish and Wildlife Service. (1995). Double-O Habitat Management Plan, Malheur National Wildlife Refuge.

US Fish and Wildlife Service. (2013). Malheur National Wildlife Refuge Comprehensive Conservation Plan. Retrieved from https://audubonportland.org/local-birding/iba/iba-map/malheur

US Fish and Wildlife Service. (2020). Habitats of Malheur. Retrieved from https://www.fws.gov/refuge/malheur/wildlife_and_habitat/habitats.html

Whittaker, J. (1990). *Graphical Models in Applied Multivariate Statistics*. John Wiley & Sons.

Wu, W. (2014). The Generalized Difference Vegetation Index (GDVI) for dryland characterization. *Remote Sensing*, *6*(2), 1211–1233. https://doi.org/10.3390/rs6021211

Zhu, Z., & Woodcock, C. E. (2012). Object-based cloud and cloud shadow detection in Landsat imagery. *Remote Sensing of Environment*, *118*, 83–94. https://doi.org/https://doi.org/10.1016/j.rse.2011.10.028

APPENDIX A. BACKGROUND AND PREVIOUS WORK ON PHREATOPHYTE RELATIONS TO GROUNDWATER

Phreatophytes in the Great Basin obtain their water requirement from surface water, groundwater, or both, through root systems that range from shallow to over 60 ft (Robinson, 1958). Phreatophytes can be classified into two categories, obligate or facultative, which relate to their levels of groundwater dependence. Obligate phreatophtyes are groundwater dependent – they only inhabit areas where they can access groundwater. Facultative phreatophytes are not solely groundwater dependent – they inhabit areas where they can access groundwater, but also inhabit areas where their water requirements can be met by precipitation derived soil moisture reserves alone. Facultative phreatophyte species common in the Great Basin include greasewood (*Sarcobatus vermiculatus*), and rabbitbrush (*Ericameria nauseous*). While these facultative phreatophyte shrub species are known to consume groundwater, studies have concluded that they primarily rely on shallow soil water derived from precipitation, and only consume harder to access groundwater during summer and early fall when shallow soil moisture levels are low (Albright et al., 2006; Chimner & Cooper, 2004; Dawson & Pate, 1996). However, a recent study in Dixie Valley, Nevada found that greasewood predominantly used groundwater throughout the entire year (Garcia et al., 2015).

Groundwater pumping for irrigation commonly results in lowering of the groundwater table (i.e. phreatic surface), leading to reduced phreatophyte groundwater evapotranspiration (ETg) and diminished vegetation vigor (Bredefoeft, 2002; Cooper et al., 2006; Elmore et al., 2003; Groeneveld et al., 2007; Naumburg et al., 2005; Patten et al., 2008). Since obligate phreatophyte species depend on groundwater, lowering of groundwater levels beyond rooting depths would likely cause a transition to a different plant community (Stromberg et al., 1996). However, since facultative phreatophyte species do not necessarily require groundwater and can survive on precipitation alone, understanding and predicting vegetation response from lowering of the shallow groundwater is more uncertain and complex than for obligate species. This uncertainty has led to detailed reviews and studies on the effects of shallow groundwater declines on phreatophyte vegetation response. Stromberg et al. (1996) found that depending upon the initial vegetation and depth to water table, a permanent water table decline could result in vegetation changing from obligate phreatophytes to facultative phreatophytes, and ultimately to non-phreatophytic upland species. Naumburg et al. (2005) reviewed past and current research at the time and concluded that additional environmental and biological factors play important roles in vegetation response to shallow groundwater level decline. Naumburg et al. (2005) developed two conceptual models to highlight these additional factors and dependencies that include the rate of groundwater level decline, soil type, potential root growth rate, and maximum potential rooting depth. Additionally, climate is identified as an important factor, specifically, precipitation timing and amount. Naumburg et al. (2005) suggest that the use of an ecological dynamics simulation model (EDYS) (Childress et al., 1999) is needed to predict vegetation response to water table fluctuations, and if these responses are gradual or threshold responses. While models such as EDYS are important and perhaps needed to potentially

identify gradual or threshold responses, a practical first step is to simply identify where vegetation response has already occurred and gather the necessary information to relate vegetation responses to changes in depth to water table and annual precipitation for example. This study highlights data collection efforts focused on remotely sensed vegetation, measured groundwater levels, and modeled climate that will ultimately help to better understand where vegetation change has already occurred, and how these changes relate to changes in groundwater levels and climate. These basic datasets can be used to provide needed information to support future prediction of phreatophyte vegetation response as a function of changes in groundwater levels, climate, and other factors.

APPENDIX B. GROUNDWATER LEVEL DATA AVAILABILITY

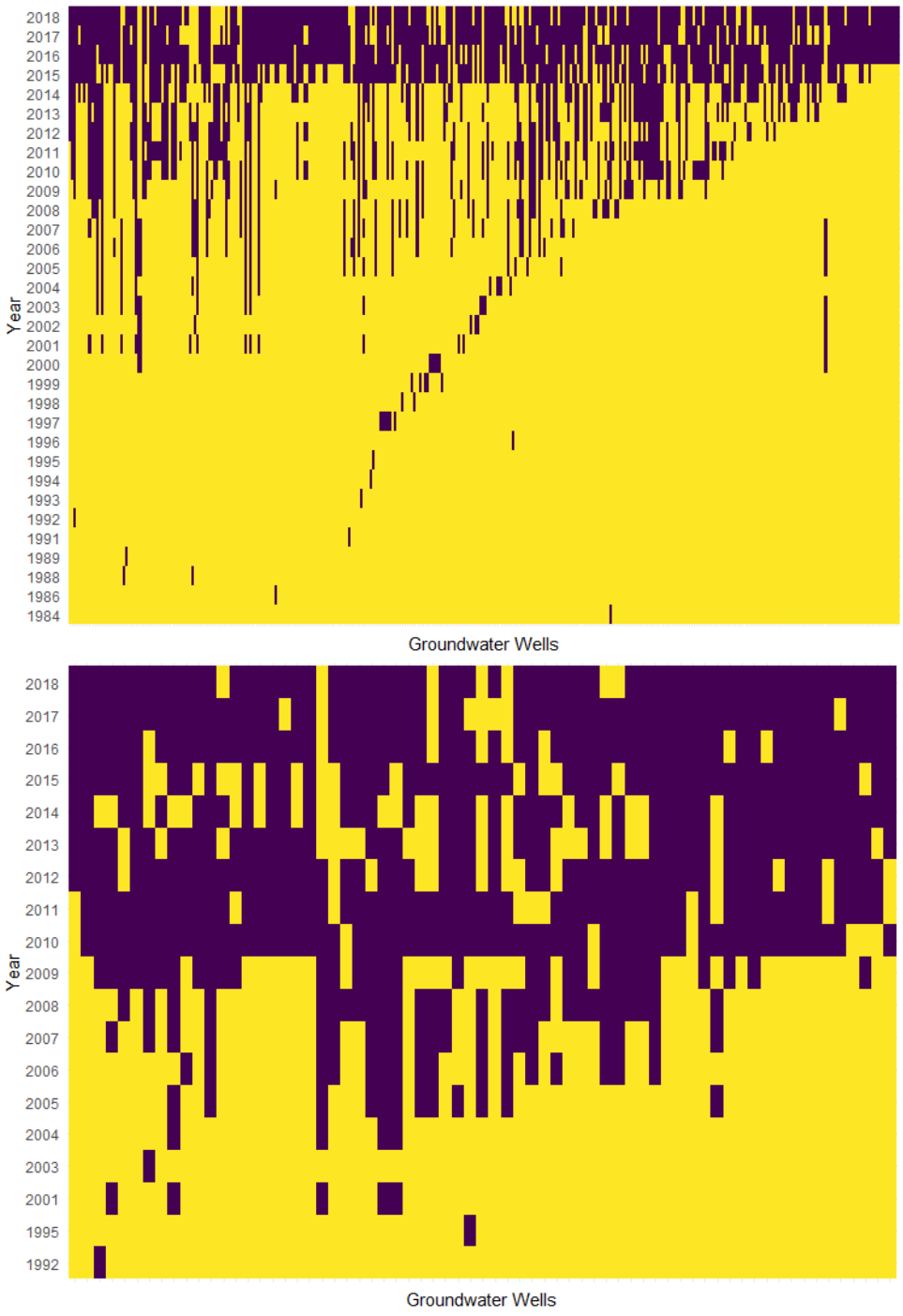

Figure B1. Overview of groundwater observation record completeness for the 1984-2018 time period for the 340 wells included in the trend analysis (upper; see Figure 3) and for the 68 wells included in the partial correlation analysis (lower; see Figures 4-5). Each column represents a single well with yellow indicating no observation for the year and dark purple indicating years when observations were available.

APPENDIX C. WELL HYDROGRAPHS

HYDROGRAPHS FOR WELLS NEAR WEST SPRINGS:

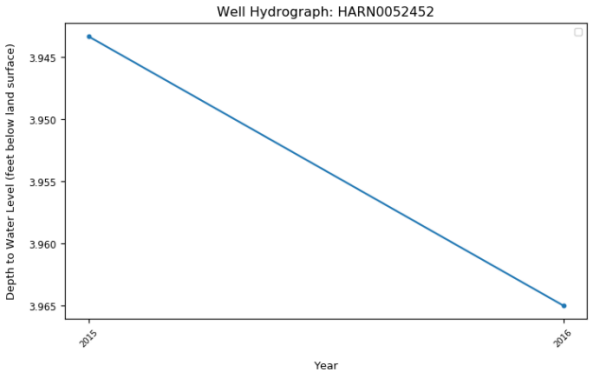

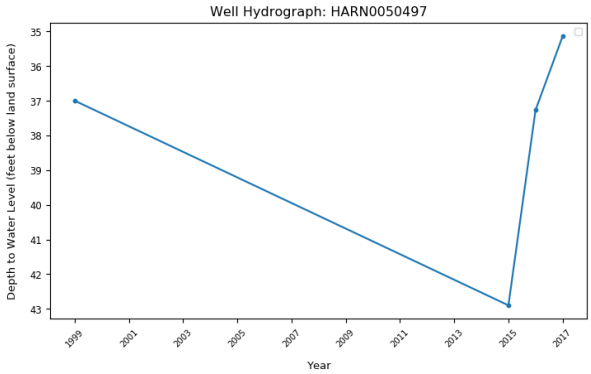

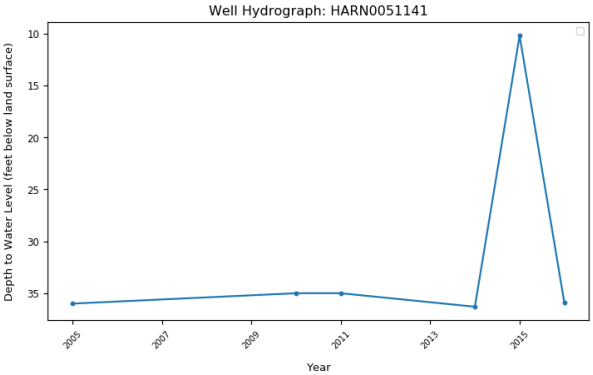

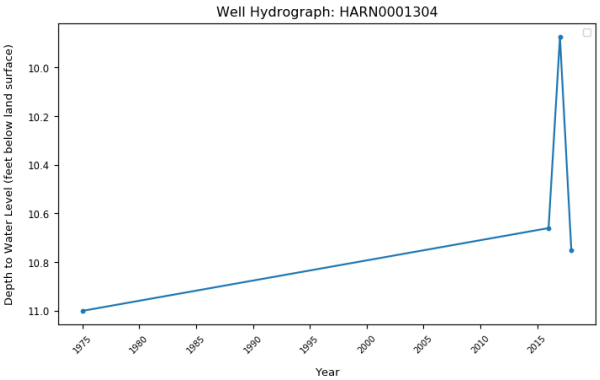

HYDROGRAPHS FOR WELLS NEAR WEAVER AND WEAVER WEST:

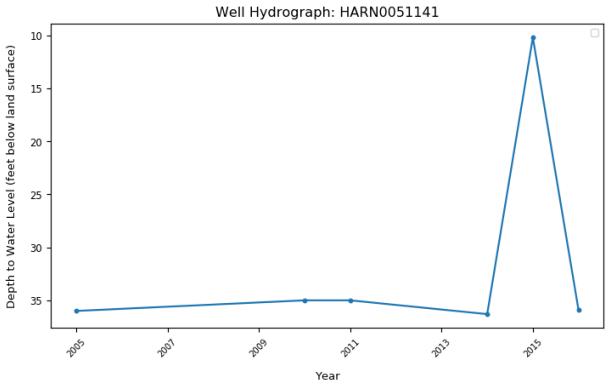

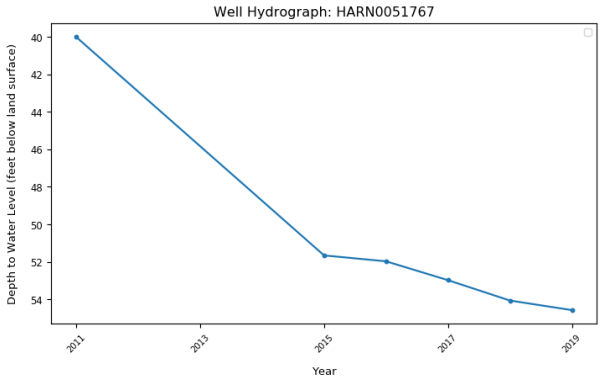

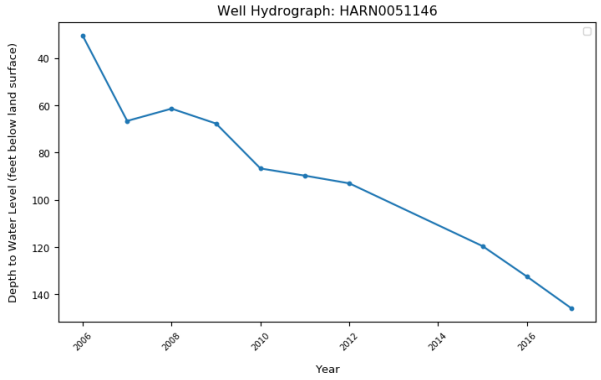

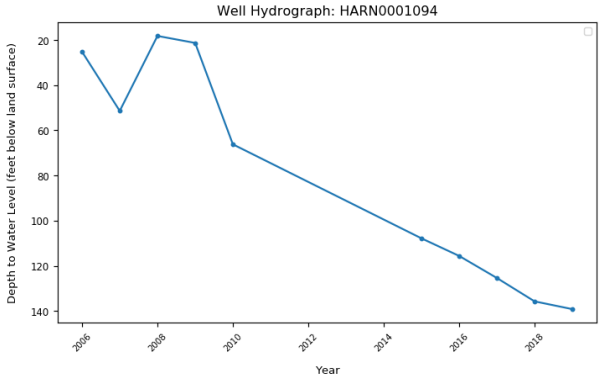

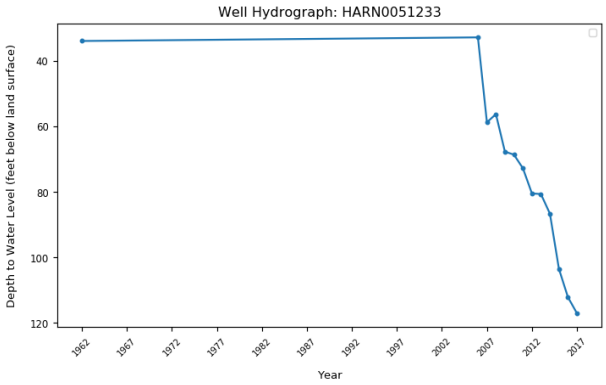
Well Hydrograph: HARN0051233
Depth to Water Level (feet below land surface)
40
60
80
100
120
1962
1967
1972
1977
1982
1987
1992
1997
2002
2007
2012
2017
Year

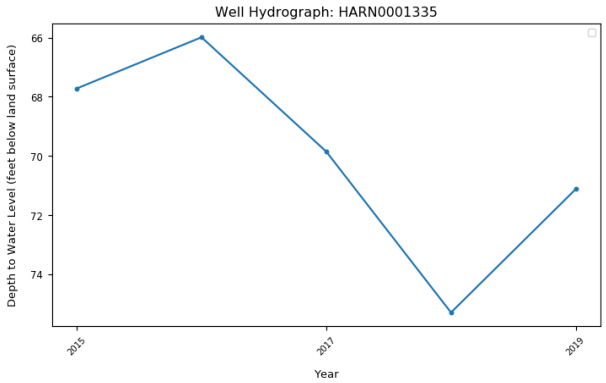
Well Hydrograph: HARN0001335
Depth to Water Level (feet below land surface)
66
68
70
72
74
2015
2017
2019
Year

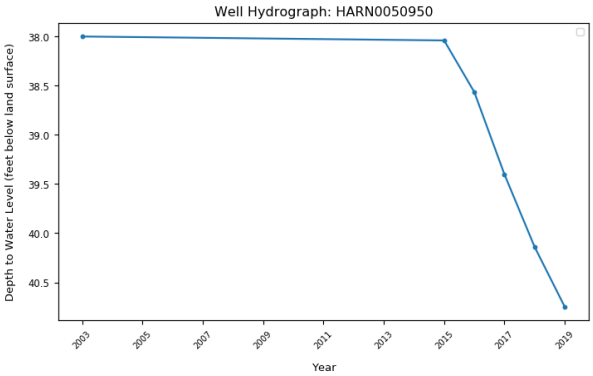
Well Hydrograph: HARN0050950
Depth to Water Level (feet below land surface)
38.0
38.5
39.0
39.5
40.0
40.5
2003
2005
2007
2009
2011
2013
2015
2017
2019
Year

HYDROGRAPHS FOR WELLS NEAR MALHEUR NORTH AND SOUTH:

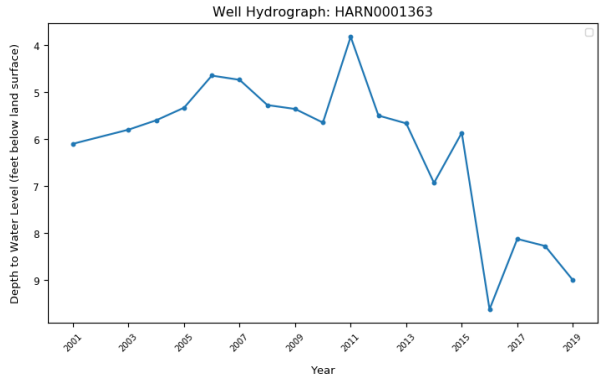

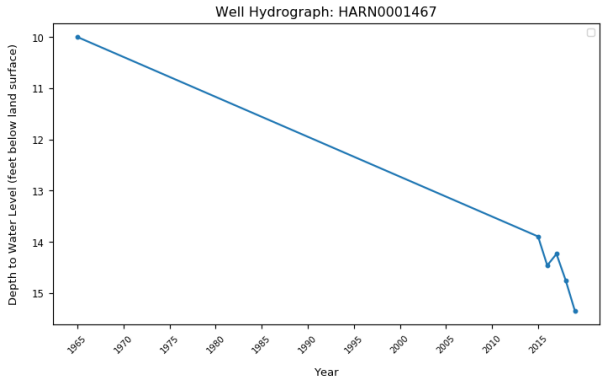

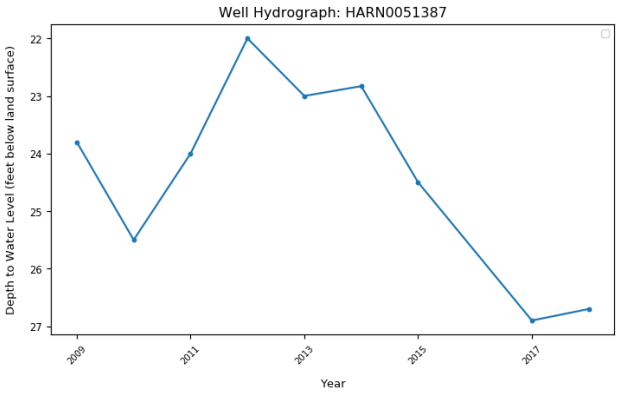

HYDROGRAPHS FOR WELLS NEAR FRENCHGLEN NORTH AND SOUTH: